also potentially could alter the responsiveness to IFN therapy. However, so far there has been no evidence of associations between polymorphisms of genes involved in type I IFN signal transduction and the efficacy of IFN therapy in patients with chronic hepatitis C.

In the present study, we examined whether single nucleotide polymorphisms (SNPs) in type I IFN signaling molecules are associated with the difference in response to IFN therapy in patients with chronic hepatitis C, using the tagging-SNP approach in a large case-control study. The tagging-SNP serves as a marker to detect associations between a particular gene region and the outcome of IFN therapy. A small set of tagging-SNPs is sufficient to capture genetic variation because polymorphisms that are physically close to each other have a tendency to be in linkage disequilibrium with each other.[14,15] The HapMap online database (http://www.hapmap.org) allows the tagging-SNP approach to be applied readily to many genes or regions.[16]

As for type I IFN signaling molecules, we focused on 2 signaling cascades downstream of type I IFN receptors. First, we examined the Janus-activated kinase (JAK)–signal transducer and activator of transcription (STAT) pathway, which is essential for type I IFN–induced antiviral activity.[17] We selected tagging-SNPs for 7 key genes in this pathway, including *IFNAR1*, *IFNAR2*, *JAK1*, tyrosine kinase 2, *STAT1*, *STAT2*, and IFN regulatory factor 9. Second, we also examined the p38 mitogen-activated protein (MAP) kinase pathway, which has been reported to cooperate with the JAK-STAT pathway in activation of type I IFN–induced antiviral activity.[18–23] We also selected tagging-SNPs for 6 key genes in this pathway, including ras-related C3 botulinum toxin substrate 1,[18] MAP kinase kinases 3 (MAPKK3),[19] *MAPKK6*,[19] p38 MAP kinase,[20,21] MAP kinase-activated protein kinase 2 (MAPKAPK2),[20–23] and *MAPKAPK3*.[20–22]

Here, we provide genetic evidence suggesting that 2 SNPs in *MAPKAPK3* are associated with the responsiveness to IFN therapy. The 2 SNPs may be useful as markers to predict the outcome of IFN therapy, which is very helpful clinically because IFN therapy is expensive and may cause serious adverse effects.[24] In addition, we provided functional evidence that suggests MAPKAPK3 influences IFN-alfa–induced antiviral activity.

Patients and Methods

Study Subjects and DNA Preparation

We enrolled 1055 patients with chronic HCV infection who were treated with IFN monotherapy before 2001, at the Department of Hepatology, Toranomon Hospital, Hiroshima University Hospital, and Hiroshima University affiliated hospitals. Each patient was treated with 6×10^6 units of IFN intramuscularly every day for 8 weeks, followed by the same dose twice a week for 16 weeks, with a total dose of 528 million units. The characteristics of participating patients are described in Table 1. All patients had abnormal serum alanine transaminase levels for more than 6 months, and were positive for both anti-HCV antibody and serum HCV RNA. All patients were negative for hepatitis B surface antigen, had no evidence of other liver diseases, and had not received immunosuppressive or antiviral therapy before enrollment in the study. Patients were classified into the following 2 groups: sustained responders (SRs) and nonresponders (NRs). SRs had normal alanine transaminase levels and no evidence of viremia at 6 months after completion of IFN therapy. Relapsed responders were excluded. NRs remained viremic at 6 months after completion of IFN therapy. HCV-RNA levels were determined by Amplicor-monitor assay (Roche Diagnostics, Basel, Switzerland) or branched-chain DNA assay and stratified into 2 categories according to cut-off values that have been reported previously.[25,26] It has been reported that having serum HCV-RNA levels higher than 1.0 mEq/mL by branched-chain DNA assay or 100 KIU/mL by Amplicor-monitor assay is a predictor of poor responsiveness to IFN therapy. Histologic staging was determined according to the previously described criteria using biopsy specimens of liver tissue.[27] All subjects in the present study were ethnically Japanese and gave written informed consent to participate in the study according to the process approved by the Ethical Committee at the SNP Research Center, The Institute of Physical and Chemical Research (RIKEN), Yokohama. Genomic DNA samples were obtained from peripheral blood of the participating pa-

Table 1. Characteristics of Patients With Chronic Hepatitis C

	SRs	NRs	*P* value
Patients, n	468	587	—
Mean age ± SD, *y*	54.6 ± 11.8	55.9 ± 10.3	.1[a]
Sex			.002
Male	325	354	
Female	143	233	
HCV genotype			<.0001[b]
1a	3	3	
1b	208	434	
2a	209	101	
2b	48	49	
HCV-RNA level[c]			<.0001[d]
High	177	420	
Low	216	69	
No data	75	98	
Fibrosis stage			.19[e]
F0	5	5	
F1	213	254	
F2	130	173	
F3	24	43	
F4	17	28	
No biopsy	79	84	

[a]Mann–Whitney U test.
[b]Chi-square test between HCV genotype 1b and non-1b.
[c]Low HCV-RNA level: <100 KIU/mL by Amplicor-monitor assay and <1.0 mEq/mL by branched-chain DNA assay.
[d]Chi-square test between HCV-RNA level high and low.
[e]Chi-square test between F0-1 and F2-4.

tients. DNA extraction was performed according to a standard phenol-chloroform protocol.[28]

Selection of Tagging-SNPs and Genotyping

As shown in Supplementary Table 1, we selected 116 tagging-SNPs for a total set of 13 candidate genes related to the type I IFN pathway, using the HapMap database (public release 21a; phase II of the January 2007 National Center for Biotechnology Information build 35 assembly; dbSNP build 125) and the Haploview program (available: http://www.broad.mit.edu/mpg/haploview). With the selection criteria of r^2 greater than 0.8 and minor allele frequency of greater than 0.05 for the Japanese population, tagging-SNPs were selected from all bins that cover the entire gene region from approximately 2000 bp upstream of the transcription start site to 1500 bp of the 3′ untranslated region in each gene. The number of tagging-SNPs in each candidate gene were as follows: *IFNAR1*, 3; *IFNAR2*, 6; *JAK1*, 8; tyrosine kinase 2, 3; *STAT1*, 23; *STAT2*, 1; IFN regulatory factor 9, 5; ras-related C3 botulinum toxin substrate 1, 7; *MAPKK3*, 5; *MAPKK6*, 35; p38 MAP kinase, 10; *MAPKAPK2*, 6; and *MAPKAPK3*, 4 (Supplementary Table 1). SNPs were genotyped by using the Invader assay[29] and the TaqMan assay[30] as described previously. The probe sets for the Invader assay were designed and synthesized by Third Wave Technologies (Madison, WI) and those for the TaqMan assay by Applied Biosystems (Foster City, CA).

SNP Discovery

To identify genetic polymorphisms within the coding region of *MAPKAPK3*, we amplified appropriate fragments of genomic DNA from 48 patients by polymerase chain reaction and sequenced the products to identify SNPs using previously described methods.[28,31]

Cells and Cell Culture

Human hepatoma cell line, Huh7, was purchased from RIKEN Cell Bank (Tsukuba, Japan). Huh7 cells were cultured in Dulbecco's modified minimal essential medium (Sigma-Aldrich, St. Louis, MO) with 10% fetal bovine serum, 100 U/mL penicillin, and 100 μg/mL streptomycin at 37°C under 5% CO_2.

Allele-Specific Transcript Quantification for MAPKAPK3

Allele-specific transcript quantification was performed as described previously,[32,33] with some modifications. Liver biopsy samples were collected from 5 patients with informed consent before IFN therapy for chronic hepatitis C. Total RNA was isolated using the RNeasy Micro kit (Qiagen, Hilden, Germany) and treated with 5 IU/mL RNase-Free DNase I (Qiagen). First-strand complementary DNA (cDNA) was prepared using the SuperScript III Platinum Two-Step quantitative reverse-transcription polymerase chain reaction kit (Invitrogen, Carlsbad, CA). Genomic DNA from peripheral blood of the 5 patients was prepared as described earlier. Both cDNA and genomic DNA were amplified with specific primers for the 3′ untranslated region of *MAPKAPK3*. The primers were as follows: forward, 5′-CCTGTGAATGCTGAGTGAGCGAGTA-3′; reverse, 5′-AGTCACCCTTTGGGTCGGGAATAGT-3′.

For determination of allele-specific *MAPKAPK3* messenger RNA (mRNA) expression, probes for SNP rs1385025 (A/G) were designed and synthesized by Third Wave Technologies. The invader assays were performed in a 5-μL reaction volume containing 1 × signal buffer, 1 × FRET Mix (FRET22/FTRE7), 30 ng cleavase VIII enzyme, 0.3 μL of probe mixture (all reagents from Third Wave Technologies), and 2 ng polymerase chain reaction product in a 96-well plate format. The thermal profile was 95°C for 5 minutes, followed by 40 cycles at 63°C for 1 minute, and a real-time intensity of fluorescence (FAM for G allele, and VIC for A of rs1385025) was measured by use of the Mx3000P Multiplex Quantitative polymerase chain reaction system (Stratagene, La Jolla, CA). For the construction of standard curves for each allele, sequential dilution of an amplified product from genomic DNA of patients with double heterozygosity for rs1385025 and rs3792323 was used. Each experiment was performed in triplicate assay at least 3 times.

Luciferase Reporter Assay

One day before transfection, 7×10^3 of Huh7 cells were seeded in a 96-well culture plate. We used 2 types of firefly luciferase expression vector that contain promoter element IFN-stimulated response element (ISRE) or IFN-γ-activated site (GAS). Huh7 cells were transfected with both 1 ng renilla luciferase expression vector pRL-TK (Promega, Madison, WI) and 10 ng firefly luciferase expression vector pISRE-TA-Luc or pGAS-TA-Luc (BD Biosciences, San Jose, CA), in conjunction with 40 ng expression plasmid pDEST51/mock (empty vector), pDEST51/*MAPKAPK3*, or pDEST51/suppressor of cytokine signaling 1, by use of the FuGENE 6 transfection reagent (Roche Applied Science, Indianapolis, IN). After 24 hours, cells were stimulated with IFN-alfa (Dainippon Sumitomo Pharma, Osaka, Japan) for 20 hours followed by Dual-Luciferase Assay (Promega). Firefly luciferase activity was normalized by renilla luciferase activity. Each experiment was performed at least 3 times. Data are expressed as mean ± SD in triplicate assay.

Statistical Analysis

We calculated allele frequencies and tested fit to Hardy-Weinberg equilibrium by the chi-square test at each SNP, using Excel software (Microsoft, Redmond, WA).[34] Then, we compared differences in genotype distribution of each SNP between cases and controls with the chi-square test and the Cochran-Armitage trend test (Excel).[35] LD coefficients (r^2) were calculated as described previously (Excel).[36] The age of the SRs and NRs was

compared by the Mann-Whitney *U* test. Differences in categoric data of patients in the 2 groups were analyzed by the chi-square test. To evaluate internal consistency of the results shown by association study, a 2-stage replication design was simulated by the Monte Carlo method. We assessed population stratification by analyzing the data from 116 tagging-SNPs in patients with HCV genotype 1b, using a genomic control method that has been reported previously.[37] Multivariate logistic regression with stepwise forward selection was performed with a significance level of 0.05 for including variables, by use of the StatFlex 5.0 software package (Artec Inc., Osaka, Japan). For case-control haplotype analysis we estimated haplotype frequencies and tested for association by chi-square analysis, to detect differences in haplotype distribution between groups we used using Haploview 3.2 software. For allele-specific transcript quantification assay, statistical differences between allelic *MAPKAPK3* mRNA expression corresponding to haplotype 1 and haplotype 2 were analyzed by Mann-Whitney *U* test. For luciferase reporter assay, comparisons among the 3 groups were analyzed by the Kruskal-Wallis test, followed by the Scheffe test to evaluate statistical differences between the 2 groups (StatFlex 5.0 software package).

Results

Association Between Tagging-SNPs in MAPKAPK3 *and the Outcome of IFN Therapy*

We searched for the association between 116 tagging-SNPs for 13 candidate genes and the outcome of IFN therapy, using 468 SR and 587 NR subjects. We were successful in genotyping all 116 tagging-SNPs (Supplementary Table 2). The mean call rate was 99.4% across all tagging-SNPs. None of the tagging-SNPs showed a significant deviation from Hardy-Weinberg equilibrium. Because HCV genotype 1b, which is the most common in Japan, is associated with poor response to IFN treatment, we divided the patients into 2 subgroups according to the genotypes of HCV with which they were infected (1b vs non-1b), and performed the comparison separately.

We found that 2 SNPs, rs3792323 (A/T) and rs616589 (G/A), located in intron 2 of MAPKAPK3, are associated with the outcome of IFN therapy in patients with HCV genotype 1b; the T allele for rs3792323 was significantly more frequent in NRs than in SRs (Table 2; 33.4% vs 22.4%; $P = 5.2 \times 10^{-5}$; odds ratio, 0.57; 95% confidence interval, 0.44-0.75). Similarly, the A allele for rs616589 was significantly more frequent in NRs than in SRs (37.8% vs 26.4%; $P = 5.6 \times 10^{-5}$; odds ratio, 0.59; 95% confidence interval, 0.45-0.76).

In Table 2, the Cochran-Armitage trend test (assuming an additive model for minor alleles) revealed an allele dose-dependent association of rs3792323 with the outcome of IFN therapy ($P = 4.6 \times 10^{-5}$), with decreased

Table 2. Associations Between the Two SNPs in *MAPKAPK3* and the Outcome of IFN Therapy

dbSNP ID	Allele 1/2	HCV genotype	Patients, n	Allele frequency, %				Genotype (%)			Cochran-Armitage trend test,	OR (95% CI)			Dominant model for allele 2 (11 vs 12, 22)			Recessive model for allele 2 (11, 12 vs 22)		
				1	2	*P* value	OR (95% CI)	11	12	22	*P* value	11 vs 12	11 vs 22		*P* value	OR (95% CI)		*P* value	OR (95% CI)	
rs3792323	A/T	total	SR (n = 468)	71.8	28.2	.088	0.85 (0.70–1.02)	242 (51.8)	187 (40.0)	38 (8.1)	.089	0.83 (0.65–1.08)	0.74 (0.47–1.15)		.10	0.82 (0.64–1.04)		.32	0.80 (0.52–1.23)	
			NR (n = 587)	68.4	31.6			273 (46.7)	253 (43.3)	58 (9.9)										
		1b	SR (n = 208)	77.6	22.4	.000052	0.57 (0.44–0.75)	124 (59.6)	75 (36.1)	9 (4.3)	.000046	0.58 (0.41–0.83)	0.30 (0.14–0.63)		.00019	0.53 (0.38–0.74)		.0074	0.38 (0.18–0.79)	
			NR (n = 434)	66.6	33.4			189 (43.9)	196 (45.5)	46 (10.7)										
		non-1b	SR (n = 260)	67.2	32.8	.056	1.36 (0.99–1.86)	118 (45.6)	112 (43.2)	29 (11.2)	.06	1.40 (0.92–2.14)	1.72 (0.83–3.57)		.067	1.45 (0.97–2.17)		.27	1.48 (0.73–2.99)	
			NR (n = 153)	73.5	26.5			84 (54.9)	57 (37.3)	12 (7.8)										
rs616589	G/A	total	SR (n = 468)	68.0	32.0	.034	0.82 (0.68–0.99)	215 (46.0)	205 (43.9)	47 (10.1)	.033	0.83 (0.64–1.07)	0.67 (0.44–1.00)		.062	0.79 (0.62–1.01)		.12	0.74 (0.50–1.08)	
			NR (n = 587)	63.6	36.4			235 (40.3)	271 (46.5)	77 (13.2)										
		1b	SR (n = 208)	73.6	26.4	.000056	0.59 (0.45–0.76)	111 (53.4)	84 (40.4)	13 (6.3)	.000048	0.59 (0.42–0.84)	0.33 (0.17–0.62)		.00023	0.53 (0.38–0.75)		.0055	0.42 (0.23–0.79)	
			NR (n = 434)	62.2	37.8			164 (38.0)	209 (48.4)	59 (13.7)										
		non-1b	SR (n = 260)	63.5	36.5	.24	1.20 (0.89–1.61)	104 (40.2)	121 (46.7)	34 (13.1)	.25	1.33 (0.87–2.05)	1.29 (0.68–2.46)		.18	1.32 (0.88–1.98)		.72	1.12 (0.61–2.06)	
			NR (n = 153)	67.5	32.5			71 (47.0)	62 (41.1)	18 (11.9)										

NOTE. *P* values were calculated from case-control analysis by the chi-square test and unadjusted for multiple testing. Odds ratios of having a sustained response to IFN therapy were calculated. Allele 1 and allele 2 denote a major and a minor allele, respectively.
OR, odds ratio; CI, confidence interval.

odds ratios of 0.58 and 0.30 for AT and TT genotypes, respectively (95% confidence interval, 0.41–0.83 for AT; 0.14–0.63 for TT). Under a dominant model for the T allele of rs3792323, a significant association also was seen in patients infected with HCV genotype 1b ($P = 1.9 \times 10^{-4}$; odds ratio, 0.53; 95% confidence interval, 0.38–0.74).

Similarly, an allele dose-dependent association of rs616589 with the responsiveness to IFN therapy was revealed in Table 2 ($P = 4.8 \times 10^{-5}$), with decreased odds ratios of 0.59 and 0.33 for GA and AA genotypes, respectively (95% confidence interval, 0.42–0.84 for GA; 0.17–0.62 for AA). Under a dominant model for the A allele of rs616589, a significant association also was seen in HCV genotype 1b–infected patients ($P = 2.3 \times 10^{-4}$; odds ratio, 0.53; 95% confidence interval, 0.38–0.75).

To adjust the P values for multiple testing, we applied a Bonferroni correction with each individual SNP as an independent variable (total, 116 SNPs). Despite this conservative adjustment, our results for rs3792323 and rs616589 about patients with HCV genotype 1b remained highly significant ($P < .05$). On the other hand, the other tagging-SNPs did not show significant associations with the outcome of IFN therapy after Bonferroni corrections (Supplementary Table 2).

Internal Validation of the Observed Associations

To evaluate internal consistency of the results shown by the association study, 2-stage replication design was simulated by the Monte Carlo method. Half of the cases and half of the controls were selected randomly from HCV-1b–infected patients in this study, and used for the first-stage test with a significance level $\alpha 1$ (the probability of making a Type I error) in the allele-frequency model. Only the SNPs that were judged to be associated significantly with the phenotype then underwent the second-stage test. In the second stage, the remaining independent cases and controls were used to test the association between the selected SNPs and the phenotype with a significance level $\alpha 2$. We set $\alpha 1$ at 0.01, 0.02, and 0.05, and calculated $\alpha 2$ as $(0.05/116)/\alpha 1$ because the global significance level after Bonferroni's correction is 0.05/116 (total, 116 SNPs). The number of iterations was 100,000 for each condition. By this method, the results of the test in the first stage are validated by the test in the second stage.

When the level of significance was set at $\alpha 1 = .01, .02$, and .05, the proportions of significant results of SNP rs3792323 were 0.563, 0.595, and 0.557, respectively (Table 3). Similarly, those of SNP rs616589 were 0.554, 0.579, and 0.540, respectively when the same values of $\alpha 1$ were used. These results suggest that the results of the first-stage test could be replicated in many cases if 2 halves of the patients, the first-stage set and the second-stage set, were tested independently for the association.

Table 3. Internal Validation Analysis of the Observed Associations Between the Two SNPs in *MAPKAPK3* and the IFN Efficacy in Patients With HCV Genotype 1b

SNP	$\alpha 1$	Proportion of significant results	95% CI
rs3792323	0.01	0.563	0.560–0.566
	0.02	0.595	0.591–0.598
	0.05	0.557	0.554–0.560
rs616589	0.01	0.554	0.551–0.557
	0.02	0.579	0.576–0.582
	0.05	0.540	0.537–0.543

$\alpha 1$, a significance level for the first-stage test; CI, confidence interval.

Population Stratification Analysis

We assessed population stratification by analyzing the data from 116 tagging-SNPs in patients with HCV genotype 1b by using the genomic control method. We estimated the inflation factor, which effectively can adjust for the confounding effect of population stratification regardless of its extent (inflation factor, 1.18; 95% confidence interval, 0.87–1.65). The corrected P values for rs3792323 and rs616589 in *MAPKAPK3* were .00017 and .00018, respectively. After a Bonferroni correction, the results for the 2 SNPs remained highly significant ($P < .05$). These results suggest that population stratification in our patients was negligible.

Haplotype Analysis

We examined whether *MAPKAPK3* haplotypes show more significant associations with the effect of IFN therapy than single-marker analysis. Because the 2 SNPs rs3792323 and rs616589 were in strong linkage disequilibrium with an r-squared value of 0.82 in our genotype data of 1055 patients, we constructed *MAPKAPK3* haplotypes from 3 tagging-SNPs (rs3792323 A>T, rs3804628 G>A, and rs2040397 C>T), using the Haploview 3.2 software. As a result, 4 haplotypes with frequencies greater than 5% were deduced in patients with HCV genotype 1b: AGC 43.9%, TGC 29.8%, AGT 20.6%, and AAC 5.7%. Although haplotype TGC was associated the most significantly with the outcome of IFN therapy in 4 haplotypes ($P = .000051$), this P value was comparable with that for single-marker analysis ($P = .000046$ for rs3792323 in the Cochran–Armitage trend test).

Results of Multivariate Logistic Regression Analysis

To determine independent factors on the outcome of IFN therapy in patients infected with HCV genotype 1b, we used multivariate logistic regression analysis with stepwise forward selection. We evaluated the following 6 factors: SNP rs3792323 (A allele vs T allele), rs616589 (G allele vs A allele), age (per year increase), sex (male vs female), fibrosis stage (F0–F1 vs F2–F4), and HCV-RNA level before treatment (low vs high).

Table 4. Predictive Factors Associated Independently With the Response to IFN Therapy in Patients With HCV Genotype 1b by Multivariate Logistic Regression Analysis

	HCV genotype 1b		
Variable	*P* value	OR	95% CI
rs3792323 (T allele/A allele)	.0011	0.29	0.14–0.61
Age (per year increase)	.0096	0.97	0.95–0.99
Fibrosis stage (F0–F1/F2–F4)	.035	1.66	1.04–2.66
HCV-RNA level (low/high)[a]	<.00001	8.25	5.05–13.50

OR, odds ratio; CI, confidence interval.
[a]Low HCV-RNA level: <100 KIU/mL by Amplicor-monitor assay and <1.0 mEq/mL by branched-chain DNA assay. Odds ratios of having a sustained response to IFN therapy were calculated.

We found that SNP rs3792323 is an independent factor associated with IFN efficacy (Table 4; $P = .0011$; odds ratio, 0.29; 95% confidence interval, 0.14–0.61). On the other hand, SNP rs616589 was removed from this model, suggesting that the 2 SNPs are not associated independently with the outcome of IFN therapy. This is consistent with the result that the 2 SNPs were in strong linkage disequilibrium in our genotype data.

Next, to eliminate the effect of confounding factors, we also tried running models by forcing in the earlier-mentioned 4 factors (age, sex, HCV-RNA level, and fibrosis stage) and SNP rs3792323 into multivariate logistic regression analysis in patients with HCV genotype 1b. We identified that SNP rs3792323 is associated with the outcome of IFN therapy ($P = .0014$; odds ratio, 0.30; 95% confidence interval, 0.14–0.63).

SNP Discovery Within the Coding Region of MAPKAPK3

To investigate whether there is any genetic polymorphism in *MAPKAPK3* that results in amino acid substitution, we sequenced the coding region of *MAPKAPK3* from genomic DNA isolated from 48 patients. We did not find any nonsynonymous allelic variants in *MAPKAPK3*.

Allele-Specific Transcript Quantification of MAPKAPK3

Next, we examined the possibility that SNP rs3792323 associates with *MAPKAPK3* expression in liver biopsy specimens from patients with chronic hepatitis C. Because rs3792323 in *MAPKAPK3* intron 2 was not present in mRNA, we selected SNP rs1385025 (A/G) in the 3′ untranslated region as a marker SNP. We confirmed that rs1385025 showed complete linkage disequilibrium to rs3792323 (D' values = 1), using HapMap data and the Haploview program. We selected 5 patients who were doubly heterozygous with genotype rs1385025 A/G and rs3792323 A/T for this assay. Haplotype pairs of these patients theoretically were specified to be haplotype 1 (rs1385025A rs3792323A) and haplotype 2 (rs1385025G rs3792323T).

We measured the relative contribution of each haplotype to *MAPKAPK3* transcription in these patients, using probes that detect each allele of rs1385025. As shown in Figure 1, allele-specific *MAPKAPK3* mRNA expression corresponding to haplotype 2 was 1.15- to 1.76-fold higher than that of haplotype 1 ($P = .009$). This result indicated that SNP rs1385025 and rs3792323 associate with the expression level of *MAPKAPK3*.

Effects of MAPKAPK3 on IFN-Alfa–Induced Gene Transcription Via ISRE and GAS Elements

We tested whether transient overexpression of MAPKAPK3 influences IFN-alfa–induced gene transcription via ISRE and GAS elements, which are essential promoter elements for type I IFN–induced antiviral activity, by use of luciferase reporter assay. When MAPKAPK3 was overexpressed in Huh7 cells, IFN-alfa–induced luciferase activities via ISRE and GAS elements were suppressed significantly by various doses of IFN-alfa, compared with the negative control (Figure 2). Similar results were obtained in suppressor of cytokine signaling 1, which has been reported to suppress IFN-alfa–induced gene expressions. In addition, we also overexpressed β-galactosidase gene as a negative control. In comparison with this control, MAPKAPK3 also significantly inhibited IFN-alfa–induced luciferase activities via ISRE and GAS elements (data not shown). These results suggest that MAPKAPK3 can inhibit IFN-alfa–induced gene transcription via ISRE and GAS elements.

Discussion

We identified that SNP rs3792323 (A/T) and rs616589 (G/A), located in *MAPKAPK3*, are associated

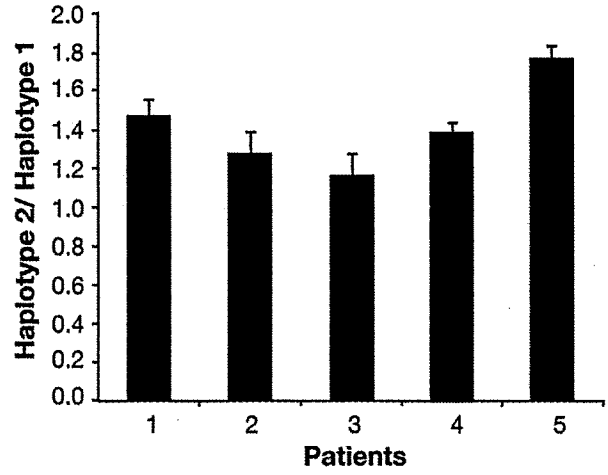

Figure 1. Allele-specific transcript quantification of *MAPKAPK3*. The allele-specific *MAPKAPK3* mRNA expression ratio for haplotype 2 to haplotype 1 is shown. Individual data from liver biopsies from 5 patients are indicated. Each experiment was performed in triplicate assay at least 3 times. Data represent the mean ± SD.

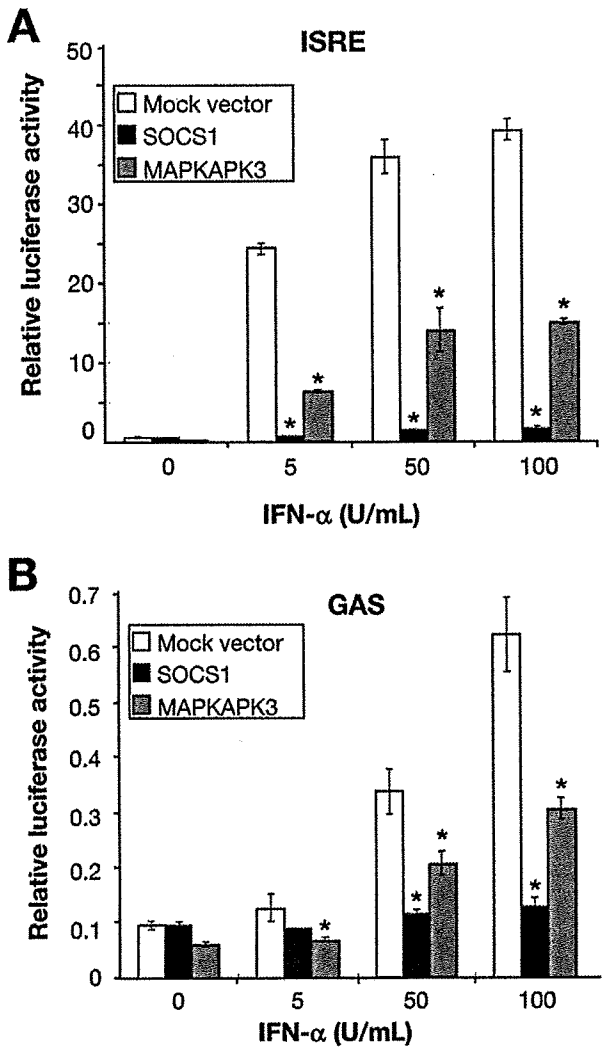

Figure 2. Effects of *MAPKAPK3* on IFN-α–induced gene transcription via ISRE and GAS elements. Huh7 cells were transfected with both 1 ng renilla luciferase expression vector pRL-TK (internal control) and 10 ng firefly luciferase expression vector (*A*) pISRE-TA-Luc or (*B*) pGAS-TA-Luc, in conjunction with 40 ng expression plasmid pDEST51/mock (negative control, *open bar*), pDEST51/suppressor of cytokine signaling 1 (SOCS1) (positive control, *black bar*), or pDEST51/*MAPKAPK3* (*gray bar*). After 24 hours, cells were stimulated with IFN-alfa for another 20 hours, and luciferase induction was measured. Firefly luciferase activity was normalized by renilla luciferase activity. Data represent the mean ± SD of triplicate assay. *$P < .05$ for comparison with mock.

with the outcome of IFN therapy in patients infected with HCV genotype 1b (Tables 2–4). In our genotype data of 1055 patients, the 2 SNPs were in strong linkage disequilibrium with an r^2 value of 0.82. Multivariate logistic regression analysis showed that rs3792323 is an independent factor associated with IFN efficacy (Table 4).

MAPKAPK3 is expressed in every human tissue.[38] *MAPKAPK3* encodes a serine/threonine-specific protein kinase and functions as a mitogen-activated protein kinase–activated protein kinase in both mitogen and stress responses.[39] MAPKAPK3 shares 72% nucleotide and 75% amino acid identity with MAPKAPK2. MAPKAPK3 and MAPKAPK2 act as downstream kinases of p38 MAP kinase under type I IFN stimulation.[22] It has been shown that disruption of p38α MAP kinase gene results in defective transcription of genes that are regulated by ISRE and GAS elements.[22] It also was reported that pharmacologic inhibition of p38 MAP kinase partially inhibits type I IFN–induced antiviral activity.[21] In mouse embryonic fibroblasts with targeted disruption of MAPKAPK2, it was indicated that type I IFN-induced antiviral activity was decreased.[22] On the other hand, little is known about the role of MAPKAPK3 in the responses to type I IFN.

In the present study, we hypothesized that enhanced expression of MAPKAPK3 is associated with resistance to IFN therapy for the following 3 reasons. First, carriers of the T allele for rs3792323, rather than the A allele, were more likely to show no response to IFN therapy (Tables 2 and 4). Thus, the T allele for rs3792323 was considered as a risk allele for nonresponse. Similarly, the A allele for rs616589 also was considered as a risk allele for nonresponse. Second, allele-specific *MAPKAPK3* mRNA expression corresponding to the T allele for rs3792323 (risk allele for nonresponse) was significantly higher than that of the A allele for rs3792323 in liver biopsy specimens of participating patients (Figure 1). Third, we did not find any nonsynonymous allelic variants in *MAPKAPK3* from the analysis of genomic DNA from 48 patients.

To examine our hypothesis, we examined whether enhanced MAPKAPK3 expression influences IFN-alfa–induced gene transcription. In reporter gene assay, overexpression of MAPKAPK3 inhibited IFN-alfa–induced gene transcription via ISRE and GAS elements (Figure 2), suggesting that MAPKAPK3 plays an important role in inhibition of IFN-α–induced antiviral activity. Several downstream effectors of MAPKAPK3 have been reported, including actin-binding protein, such as heat shock protein 27,[39] and transcription factors such as basic helix-loop-helix transcription factor E47[40] and cyclic AMP responsive element binding protein.[41] However, the mechanisms by which MAPKAPK3 inhibits IFN-α–induced gene transcription still are unclear, and further investigations are required. It also is interesting to examine the allele-specific *MAPKAPK3* mRNA levels during interferon therapy. Although we have no direct information, MAPKAKP3 mRNA expression is not inducible by IFN-alfa stimulation in human hepatoma cell line Huh-7 and HepG2 (data not shown).

In this study, the association between the *MAPKAPK3* polymorphisms and the efficacy of IFN therapy was observed in HCV genotype 1b, but not found in genotype non-1b. The reason for this difference between the 2 groups is yet to be seen. As one possible reason, the high susceptibility of genotype non-1b to IFN treatment may make the fine effect of SNPs obscure. As another possible

explanation, the effect of MAPKAPK3 on IFN efficacy may vary among different HCV genotypes. It was reported that associations between SNPs in the osteopontin gene and the efficacy of IFN therapy were particularly evident in patients with genotype 1b and a high virus titer, rather than in patients with genotype non-1b.[26] Until now, in various HCV genotypes including 1a, 1b, and 2a, HCV subgenomic replicon cell lines, which show autonomous HCV-RNA replication in the human hepatoma cell line, have been established. In the case that MAPKAPK3 is overexpressed in these HCV replicon cell lines, it is interesting to examine whether the effect of MAPKAPK3 on IFN efficacy is different or not among these HCV genotypes. It also is important to test associations between the *MAPKAPK3* SNPs and the IFN efficacy in each subgroup of patients infected with each HCV genotype including 1a, 2a, and 2b.

Recently, it was reported that the combination treatment of IFN-alfa plus ribavirin results in higher rates of sustained response than IFN monotherapy.[2,3] Various mechanisms of ribavirin activity against HCV have been proposed.[42] However, it is notable that treatment with ribavirin alone has no effect on serum HCV-RNA level.[43,44] On the other hand, the addition of ribavirin to IFN-alfa monotherapy leads to marked reduction of the serum HCV-RNA level. These facts suggest that IFN-alfa signaling is important for the induction of antiviral activity not only in IFN-alfa monotherapy but also in IFN-alfa combination therapy with ribavirin. Therefore, it is likely that the inhibitory effect of MAPKAPK3 on IFN signaling influences the efficacy of IFN-alfa combination therapy as well as IFN-alfa monotherapy. At present, about 50% of patients infected with HCV genotype 1b fail to eradicate the virus even after combination therapy of IFN-α plus ribavirin.[1–3] It is important to examine whether the 2 SNPs are associated with the responsiveness to combination therapy of IFN-alfa plus ribavirin.

It remains to be seen whether or not rs3792323 and rs616589 are functional cis-acting polymorphisms affecting *MAPKAPK3* expression. Even if the 2 SNPs do not have functional effects, it is expected that the 2 SNPs can serve as marker SNPs in linkage disequilibrium with functional cis-acting polymorphisms.[45] Furthermore, the 2 SNPs may be useful as genetic markers to predict the efficacy of IFN therapy. In our patients with IFN-alfa monotherapy, patients with risk alleles for nonresponse (T allele for rs3792323, A allele for rs616589) were more likely to be NRs compared with risk allele–negative patients (Tables 2 and 4). Although the results of our internal validation suggest that the observed association between the 2 SNPs in *MAPKAPK3* and the IFN efficacy is internally consistent, further replication with an independent cohort is needed to confirm the association. It also is interesting to test associations between the 2 SNPs and the phenotypes in relapsed patients. At present, we do not enroll enough of these patients to examine the association. In the future, we will enroll enough patients and test the association.

It was reported that polymorphism of GT-repeat length in the IFNAR1 promoter region was associated with the outcome of IFN therapy for chronic HCV infection in a study of 157 Japanese patients (HCV genotype total, $P = .008$).[13] In our study, we could not find a similar association for analyzed tagging-SNPs in IFNAR1 (Supplementary Table 2). The reason for the discrepancy between the 2 studies is not clear at present. Unfortunately, the GT-repeat polymorphism in IFNAR1 is not included in the HapMap database. Therefore, it is not clear whether tagging-SNPs have strong linkage disequilibrium with the GT-repeat polymorphism in IFNAR1. Possibly, tagging-SNPs may not capture the GT-repeat polymorphism in IFNAR1. To explain the discrepancy between the present study and the previous study, it is desirable to genotype the GT-repeat polymorphism in IFNAR1 by direct sequencing.

In conclusion, we identified that SNP rs3792323 in *MAPKAPK3* is associated strongly with the outcome of IFN therapy in patients infected with HCV genotype 1b. In addition, we showed that SNP rs3792323 associates with the expression level of *MAPKAPK3* and *MAPKAPK3* inhibits IFN-alfa–induced gene transcription via ISRE and GAS elements. Therefore, MAPKAPK3 may play an important role in the inhibition of IFN-alfa–induced antiviral activity.

Supplementary Data

Note: To access the supplementary material accompanying this article, visit the online version of *Gastroenterology* at www.gastrojournal.org, and at doi: 10.1053/j.gastro.2009.01.061.

Appendix

The authors thank the other members of the SNP Research Center for assistance with various aspects of this study.

Hiroshima Liver Study Group

Dr Tsuge and Dr Chayama are members of the Hiroshima Liver Study Group. Other members (listed in alphabetical order) include Hiroshi Aikata (Hiroshima University, Hiroshima, Japan), Shiomi Aimitsu (Hiroshima Red Cross Hospital, Hiroshima, Japan), Yasuyuki Aisaka (Hiroshima Red Cross Hospital, Hiroshima, Japan), Hajime Amano (Onomichi General Hospital, Hiroshima, Japan), Tatsuya Amimoto (Amimoto Clinic, Hiroshima, Japan), Keiko Arataki (Hiroshimakinen Hospital, Hiroshima, Japan), Nobuyuki Asada (Asada Clinic, Hiroshima, Japan), Takahiro Azakami (Hiroshima University, Hiroshima, Japan), Nobuhiko Hiraga (Hiroshima University, Hiroshima, Japan), Akira Hiramatsu (Chuden Hospital, Hiroshima, Japan), Hideyuki Hyogo (Hiroshima

University, Hiroshima, Japan), Michio Imamura (Hiroshima University, Hiroshima, Japan), Kunio Ishida (Hiroshima General Hospital, Hiroshima, Japan), Hiroto Ishihara (Chuden Hospital, Hiroshima, Japan), Tomokazu Ishitobi (Hiroshima University, Hiroshima, Japan), Hiroyuki Ito (Saiseikai Kure Hospital, Hiroshima, Japan), Keiko Iwamoto (Hiroshima University, Hiroshima, Japan), Soo Cheol Jeong (Hiroshima University, Hiroshima, Japan), Koji Kamada (Shobara Red Cross Hospital, Hiroshima, Japan), Masaya Kamiyasu (Kamiyasu Clinic, Hiroshima, Japan), Yoshio Katamura (Hiroshima University, Hiroshima, Japan), Hiroiku Kawakami (Kawakami Clinic, Hiroshima, Japan), Yoshiiku Kawakami (Hiroshima University, Hiroshima, Japan), Masahiro Kawanishi (Higashihiroshima Medical Center, Hiroshima, Japan), Tomokazu Kawaoka (Hiroshima University, Hiroshima, Japan), Takashi Kimura (Hiroshima University, Hiroshima, Japan), Shinsuke Kira (Hiroshima Red Cross Hospital, Hiroshima, Japan), Mikiya Kitamoto (Hiroshima Prefectural Hospital, Hiroshima, Japan), Hideaki Kodama (Saiseikai Hiroshima Hospital, Hiroshima, Japan), Hiroshi Kohno (Kure Medical Center, Hiroshima, Japan), Hirotaka Kohno (Kure Medical Center, Hiroshima, Japan), Toshiyuki Masanaga (Masanaga Clinic, Hiroshima, Japan), Akiko Matsumoto (Hiroshima Mitsubishi Hospital, Hiroshima, Japan), Daiki Miki (Hiroshima University, Hiroshima, Japan), Fukiko Mitsui (Hiroshima University, Hiroshima, Japan), Toshio Miura (Akitsu Prefectural Hospital, Hiroshima, Japan), Nami Mori (Hiroshima University, Hiroshima, Japan), Takashi Moriya (Chugoku Rousai Hospital, Hiroshima, Japan), Yutaka Nabeshima (Hiroshima University, Hiroshima, Japan), Toshio Nakamura (Nakamura Clinic, Hiroshima, Japan), Toshio Nakanishi (Shobara Red Cross Hospital, Hiroshima, Japan), Ryo Nakashio (Nakashio Clinic, Hiroshima, Japan), Michihiro Nanaka (Hiroshima University, Hiroshima, Japan), Makoto Ohbayashi (Onomichi General Hospital, Hiroshima, Japan), Waka Ohishi (Radiation Effects Research Foundation, Hiroshima, Japan), Shigeo Orime (Chuden Hospital, Hiroshima, Japan), Hiromi Saneto (Hiroshima University, Hiroshima, Japan), Hiroo Shirakawa (Funairi Hospital, Hiroshima, Japan), Shoichi Takahashi (Hiroshima University, Hiroshima, Japan), Shintaro Takaki (Hiroshima University, Hiroshima, Japan), Eichi Takesaki (Higashihiroshima Medical Center, Hiroshima, Japan), Toru Tamura (Mazda Hospital, Hiroshima, Japan), Keiji Tsuji (Hiroshima City Asa Hospital, Hiroshima, Japan), Kiminori Uka (Hiroshima University, Hiroshima, Japan), Koji Waki (Saiseikai Hiroshima Hospital, Hiroshima, Japan), Masashi Watanabe (Kuchiwa Clinic, Hiroshima, Japan), Syuji Yamaguchi (Kure Kyosai Hospital, Hiroshima, Japan), Keitaro Yamashina (Hiroshima General Hospital of West Japan Railway Company, Hiroshima, Japan), Hitoshi Yokoya (Fuchu Kita Hospital, Hiroshima, Japan), and Tatsuji Yokoyama (Takanobashi Central Hospital, Hiroshima, Japan).

Toranomon Hospital

Dr Kumada is a member of the Department of Hepatology, Toranomon Hospital. Other members (listed in alphabetical order) include Norio Akuta, Yasuji Arase, Miharu Hirakawa, Tetsuya Hosaka, Kenji Ikeda, Yusuke Kawamura, Mariko Kobayashi, Masahiro Kobayashi, Satoshi Saitoh, Hitomi Sezaki, Yoshiyuki Suzuki, Fumitaka Suzuki, and Hiromi Yatsuji.

BASIC-LIVER, PANCREAS, AND BILIARY TRACT

References

1. Fried MW, Shiffman ML, Reddy KR, et al. Peginterferon alfa-2a plus ribavirin for chronic hepatitis C virus infection. N Engl J Med 2002;347:975–982.
2. Management of hepatitis C. NIH Consensus Statement 1997; available at http://consensus.nih.gov/1997/1997HepatitisC105html.htm.
3. Liang TJ, Rehermann B, Seeff LB, et al. Pathogenesis, natural history, treatment, and prevention of hepatitis C. Ann Intern Med 2000;132:296–305.
4. Martinot-Peignoux M, Marcellin P, Pouteau M, et al. Pretreatment serum hepatitis C virus RNA levels and hepatitis C virus genotype are the main and independent prognostic factors of sustained response to interferon alfa therapy in chronic hepatitis C. Hepatology 1995;22:1050–1056.
5. Trepo C. Genotype and viral load as prognostic indicators in the treatment of hepatitis C. J Viral Hepat 2000;7:250–257.
6. Walsh MJ, Jonsson JR, Richardson MM, et al. Non-response to antiviral therapy is associated with obesity and increased hepatic expression of suppressor of cytokine signalling 3 (SOCS-3) in patients with chronic hepatitis C, viral genotype 1. Gut 2006;55:529–535.
7. Gao B, Hong F, Radaeva S. Host factors and failure of interferon-alpha treatment in hepatitis C virus. Hepatology 2004;39:880–890.
8. Huang Y, Yang H, Borg BB, et al. A functional SNP of interferon-gamma gene is important for interferon-alpha-induced and spontaneous recovery from hepatitis C virus infection. Proc Natl Acad Sci U S A 2007;104:985–990.
9. Yee LJ, Tang J, Gibson AW, et al. Interleukin 10 polymorphisms as predictors of sustained response in antiviral therapy for chronic hepatitis C infection. Hepatology 2001;33:708–712.
10. Naito M, Matsui A, Inao M, et al. SNPs in the promoter region of the osteopontin gene as a marker predicting the efficacy of interferon-based therapies in patients with chronic hepatitis C. J Gastroenterol 2005;40:381–388.
11. Suzuki F, Arase Y, Suzuki Y, et al. Single nucleotide polymorphism of the MxA gene promoter influences the response to interferon monotherapy in patients with hepatitis C viral infection. J Viral Hepat 2004;11:271–276.
12. Vidigal PG, Germer JJ, Zein NN. Polymorphisms in the interleukin-10, tumor necrosis factor-alpha, and transforming growth factor-beta1 genes in chronic hepatitis C patients treated with interferon and ribavirin. J Hepatol 2002;36:271–277.
13. Matsuyama N, Mishiro S, Sugimoto M, et al. The dinucleotide microsatellite polymorphism of the IFNAR1 gene promoter correlates with responsiveness of hepatitis C patients to interferon. Hepatol Res 2003;25:221–225.
14. Pharoah PD, Dunning AM, Ponder BA, et al. Association studies for finding cancer-susceptibility genetic variants. Nat Rev Cancer 2004;4:850–860.

15. Johnson GC, Esposito L, Barratt BJ, et al. Haplotype tagging for the identification of common disease genes. Nat Genet 2001; 29:233–237.
16. Gibbs RA, Belmont JW, Hardenbol P, et al. The International HapMap Project. Nature 2003;426:789–796.
17. Darnell JE Jr, Kerr IM, Stark GR. Jak-STAT pathways and transcriptional activation in response to IFNs and other extracellular signaling proteins. Science 1994;264:1415–1421.
18. Uddin S, Lekmine F, Sharma N, et al. The Rac1/p38 mitogen-activated protein kinase pathway is required for interferon alpha-dependent transcriptional activation but not serine phosphorylation of Stat proteins. J Biol Chem 2000;275:27634–27640.
19. Li Y, Batra S, Sassano A, et al. Activation of mitogen-activated protein kinase kinase (MKK) 3 and MKK6 by type I interferons. J Biol Chem 2005;280:10001–10010.
20. Uddin S, Majchrzak B, Woodson J, et al. Activation of the p38 mitogen-activated protein kinase by type I interferons. J Biol Chem 1999;274:30127–30131.
21. Mayer IA, Verma A, Grumbach IM, et al. The p38 MAPK pathway mediates the growth inhibitory effects of interferon-alpha in BCR-ABL-expressing cells. J Biol Chem 2001;276:28570–28577.
22. Li Y, Sassano A, Majchrzak B, et al. Role of p38alpha Map kinase in type I interferon signaling. J Biol Chem 2004;279:970–979.
23. Ishida H, Ohkawa K, Hosui A, et al. Involvement of p38 signaling pathway in interferon-alpha-mediated antiviral activity toward hepatitis C virus. Biochem Biophys Res Commun 2004;321:722–727.
24. Hoofnagle JH. Therapy of acute and chronic viral hepatitis. Adv Intern Med 1994;39:241–275.
25. Shiratori Y, Kato N, Yokosuka O, et al. Predictors of the efficacy of interferon therapy in chronic hepatitis C virus infection. Tokyo-Chiba Hepatitis Research Group. Gastroenterology 1997;113: 558–566.
26. Naito M, Matsui A, Inao M, et al. SNPs in the promoter region of the osteopontin gene as a marker predicting the efficacy of interferon-based therapies in patients with chronic hepatitis C. J Gastroenterol 2005;40:381–388.
27. Desmet VJ, Gerber M, Hoofnagle JH, et al. Classification of chronic hepatitis: diagnosis, grading and staging. Hepatology 1994;19:1513–1520.
28. Ozaki K, Ohnishi Y, Iida A, et al. Functional SNPs in the lymphotoxin-alpha gene that are associated with susceptibility to myocardial infarction. Nat Genet 2002;32:650–654.
29. Ohnishi Y, Tanaka T, Ozaki K, et al. A high-throughput SNP typing system for genome-wide association studies. J Hum Genet 2001; 46:471–477.
30. Suzuki A, Yamada R, Chang X, et al. Functional haplotypes of PADI4, encoding citrullinating enzyme peptidylarginine deiminase 4, are associated with rheumatoid arthritis. Nat Genet 2003;34: 395–402.
31. Iida A, Saito S, Sekine A, et al. Catalog of 258 single-nucleotide polymorphisms (SNPs) in genes encoding three organic anion transporters, three organic anion-transporting polypeptides, and three NADH:ubiquinone oxidoreductase flavoproteins. J Hum Genet 2001;46:668–683.
32. Osawa N, Koya D, Araki S, et al. Combinational effect of genes for the renin-angiotensin system in conferring susceptibility to diabetic nephropathy. J Hum Genet 2007;52:143–151.
33. Kamiyama M, Kobayashi M, Araki SI, et al. Polymorphisms in the 3′ untranslated region in the neurocalcin delta gene affect mRNA stability, and confer susceptibility to diabetic nephropathy. Hum Genet 2007;122:397–407.
34. Nielsen DM, Ehm MG, Weir BS. Detecting marker-disease association by testing for Hardy-Weinberg disequilibrium at a marker locus. Am J Hum Genet 1998;63:1531–1540.
35. Sladek R, Rocheleau G, Rung J, et al. A genome-wide association study identifies novel risk loci for type 2 diabetes. Nature 2007; 445:881–885.
36. Devlin B, Risch N. A comparison of linkage disequilibrium measures for fine-scale mapping. Genomics 1995;29:311–322.
37. Freedman ML, Reich D, Penney KL, et al. Assessing the impact of population stratification on genetic association studies. Nat Genet 2004;36:388–393.
38. Sithanandam G, Latif F, Duh FM, et al. 3pK, a new mitogen-activated protein kinase-activated protein kinase located in the small cell lung cancer tumor suppressor gene region. Mol Cell Biol 1996;16:868–876.
39. Ludwig S, Engel K, Hoffmeyer A, et al. 3pK, a novel mitogen-activated protein (MAP) kinase-activated protein kinase, is targeted by three MAP kinase pathways. Mol Cell Biol 1996;16: 6687–6697.
40. Neufeld B, Grosse-Wilde A, Hoffmeyer A, et al. Serine/threonine kinases 3pK and MAPK-activated protein kinase 2 interact with the basic helix-loop-helix transcription factor E47 and repress its transcriptional activity. J Biol Chem 2000;275:20239–20242.
41. Maizels ET, Mukherjee A, Sithanandam G, et al. Developmental regulation of mitogen-activated protein kinase-activated kinases-2 and -3 (MAPKAPK-2/-3) in vivo during corpus luteum formation in the rat. Mol Endocrinol 2001;15:716–733.
42. Feld JJ, Hoofnagle JH. Mechanism of action of interferon and ribavirin in treatment of hepatitis C. Nature 2005;436:967–972.
43. Lau JY, Tam RC, Liang TJ, et al. Mechanism of action of ribavirin in the combination treatment of chronic HCV infection. Hepatology 2002;35:1002–1009.
44. Hoofnagle JH, Lau D, Conjeevaram H, et al. Prolonged therapy of chronic hepatitis C with ribavirin. J Viral Hepat 1996;3:247–252.
45. Gabriel SB, Schaffner SF, Nguyen H, et al. The structure of haplotype blocks in the human genome. Science 2002;296: 2225–2229.

Received January 03, 2008. Accepted January 29, 2009.

Reprint requests

Address requests for reprints to: Kazuaki Chayama, MD, PhD, Laboratory for Digestive Diseases, Center for Genomic Medicine, RIKEN (The Institute of Physical and Chemical Research), 1-2-3 Kasumi, Minami-ku, Hiroshima 734-8551, Japan. e-mail: chayama@hiroshima-u.ac.jp; fax: (81) 82-255-6220.

Acknowledgment

The authors thank the patients who generously agreed to participate in this study. The authors also thank the team members at the Department of Hepatology, Toranomon Hospital, Hiroshima University Hospital, and Hiroshima Liver Study Group for clinical sample collection. The authors acknowledge Dr N. Osawa and Dr Y. Nagasaka for helpful discussion; and Y. Kikuchi, M. Habata, M. Yahata, and T. Hirooka for technical assistance.

Conflicts of interest

The authors disclose no conflicts.

Funding

This study was supported by a grant from the Japanese Millennium Project, and in part by Dainippon Sumitomo Pharma Co, Ltd. This work was also supported in part by a Grant-in-Aid for Scientific Research and Development from the Ministry of Education, Sports, Culture, and Technology and the Ministry of Health, Labor, and Welfare.

Supplementary Table 1. Candidate Genes Related to Type I IFN Pathway and Selected 116 Tagging-SNPs

dbSNP ID	Gene symbol	Alleles	SNP bin	SNP location
rs2243594	*IFNAR1*	A/G	Bin1	Intron2_108
rs2243600	*IFNAR1*	G/T	Bin2	Intron8_1812
rs2252930	*IFNAR1*	C/G	Bin3	Intron1_6765
rs2252650	*IFNAR2*	A/T	Bin1	Intron4_571
rs6517154	*IFNAR2*	T/C	Bin2	Intron1_6159
rs2073362	*IFNAR2*	A/G	Bin3	Intron5_1606
rs2248202	*IFNAR2*	A/C	Bin4	Intron1_1359
rs10211925	*IFNAR2*	G/A	Bin5	Intron2_1450
rs2248412	*IFNAR2*	A/G	Bin7	Intron1_3010
rs310209	*JAK1*	C/A	Bin1	Intron2_3344
rs3790541	*JAK1*	C/T	Bin2	Intron3_3141
rs310247	*JAK1*	A/G	Bin3	Intron16_2338
rs3790532	*JAK1*	G/A	Bin4	Intron21_225
rs2254002	*JAK1*	A/C	Bin5	Intron22_112
rs3818753	*JAK1*	A/G	Bin6	Intron3_5476
rs17127024	*JAK1*	G/T	Bin7	Intron21_484
rs2274948	*JAK1*	T/C	Bin8	Intron9_1930
rs280523	Tyrosine kinase2	G/A	Bin1	Exon6_51
rs280519	Tyrosine kinase2	A/G	Bin2	Intron11_7
rs280496	Tyrosine kinase2	C/G	Bin3	Intron22_122
rs11885069	*STAT1*	C/T	Bin1	Intron5_1665
rs9789428	*STAT1*	C/A	Bin2	Intron21_656
rs2280233	*STAT1*	T/C	Bin3	Intron14_1014
rs13395505	*STAT1*	A/G	Bin4	3′flank_1750
rs12693589	*STAT1*	C/T	Bin5	3′flank_7602
rs2066805	*STAT1*	T/C	Bin6	Intron8_42
rs1400657	*STAT1*	T/G	Bin7	3′flank_6724
rs3771300	*STAT1*	T/G	Bin8	3′flank_4668
rs11677408	*STAT1*	C/T	Bin9	Intron5_5674
rs11887698	*STAT1*	A/G	Bin10	Intron11_1080
rs2030171	*STAT1*	A/G	Bin11	Intron5_3126
rs1467199	*STAT1*	C/G	Bin12	5′flank_-1566
rs10199181	*STAT1*	T/A	Bin13	Intron4_136
rs2066802	*STAT1*	A/G	Bin15	Exon3_64
rs16833155	*STAT1*	C/T	Bin16	Intron9_1205
rs2066799	*STAT1*	C/T	Bin17	Intron14_95
rs11693463	*STAT1*	A/G	Bin18	Intron5_2378
rs10208033	*STAT1*	C/T	Bin19	5′flank_-481
rs3755312	*STAT1*	C/G	Bin20	Intron18_1118
rs2280232	*STAT1*	A/C	Bin21	Intron14_814
rs13029532	*STAT1*	A/C	Bin22	Intron2_2350
rs7562024	*STAT1*	T/C	Bin23	Intron11_433
rs1914408	*STAT1*	C/T	Bin24	3′flank_288
rs2066807	*STAT2*	C/G	Bin1	Exon20_58
rs12432194	IFN regulatory factor 9	C/T	Bin1	3′flank_251
rs4981494	IFN regulatory factor 9	G/A	Bin2	5′flank_-331
rs12432304	IFN regulatory factor 9	C/T	Bin3	3′flank_1029
rs2277484	IFN regulatory factor 9	G/A	Bin4	5′flank_-678
rs2236350	IFN regulatory factor 9	C/A	Bin5	Intron1_463
rs2303364	Ras-related C3 botulinum toxin substrate 1	C/T	Bin1	Intron6_30
rs836483	Ras-related C3 botulinum toxin substrate 1	G/A	Bin2	Intron3_827
rs6954996	Ras-related C3 botulinum toxin substrate 1	G/A	Bin3	Intron5_1439
rs7456834	Ras-related C3 botulinum toxin substrate 1	G/C	Bin4	Intron2_1041
rs702484	Ras-related C3 botulinum toxin substrate 1	G/C	Bin5	Intron4_261
rs2347339	Ras-related C3 botulinum toxin substrate 1	C/G	Bin6	Intron2_8177
rs768409	Ras-related C3 botulinum toxin substrate 1	A/T	Bin7	Intron1_9471
rs2305871	*MAPKK3*	G/C	Bin1	Intron6_35
rs9901404	*MAPKK3*	G/A	Bin2	3′flank_5917
rs12602109	*MAPKK3*	G/A	Bin3	3′flank_8737
rs3760201	*MAPKK3*	A/G	Bin4	Intron1_5337
rs8074866	*MAPKK3*	C/T	Bin5	Intron1_2246
rs2074028	*MAPKK6*	T/C	Bin1	Intron7_308
rs2034100	*MAPKK6*	G/A	Bin2	Intron1_1022

Supplementary Table 1. (Continued)

dbSNP ID	Gene symbol	Alleles	SNP bin	SNP location
rs817565	*MAPKK6*	T/G	Bin3	Intron1_21244
rs2251862	*MAPKK6*	C/A	Bin4	Exon3_8
rs2072073	*MAPKK6*	C/G	Bin5	3′flank_500
rs2716213	*MAPKK6*	T/G	Bin6	Intron1_86422
rs12451722	*MAPKK6*	T/C	Bin7	Intron1_23084
rs6501326	*MAPKK6*	A/G	Bin8	Intron1_31727
rs2716225	*MAPKK6*	G/A	Bin9	Intron1_56816
rs8080760	*MAPKK6*	A/G	Bin10	Intron1_45400
rs12948059	*MAPKK6*	A/G	Bin11	Intron1_83353
rs2074027	*MAPKK6*	A/G	Bin12	Intron2_151
rs2716222	*MAPKK6*	C/T	Bin13	Intron1_75110
rs4968857	*MAPKK6*	T/C	Bin14	Intron1_9292
rs756944	*MAPKK6*	T/C	Bin15	Intron10_8385
rs2715806	*MAPKK6*	G/A	Bin16	Intron1_48526
rs8078890	*MAPKK6*	A/C	Bin17	Intron1_71173
rs2716191	*MAPKK6*	C/T	Bin18	Intron11_4021
rs2715812	*MAPKK6*	C/T	Bin19	Intron1_57430
rs11869073	*MAPKK6*	A/C	Bin20	Intron1_65672
rs12945375	*MAPKK6*	A/G	Bin21	Intron1_58307
rs12939509	*MAPKK6*	A/G	Bin22	Intron1_38245
rs8082399	*MAPKK6*	G/A	Bin23	Intron1_3166
rs2716195	*MAPKK6*	G/A	Bin24	Intron10_5581
rs2716223	*MAPKK6*	G/A	Bin25	Intron1_75080
rs2715810	*MAPKK6*	G/A	Bin26	Intron1_40643
rs7213686	*MAPKK6*	T/C	Bin27	Intron1_42333
rs8067307	*MAPKK6*	C/A	Bin28	Intron10_5994
rs4968859	*MAPKK6*	A/C	Bin29	Intron1_47927
rs9893349	*MAPKK6*	G/A	Bin30	Intron1_62870
rs17690015	*MAPKK6*	G/A	Bin31	Intron1_51658
rs2715834	*MAPKK6*	G/C	Bin32	Intron10_5872
rs1548444	*MAPKK6*	T/G	Bin33	Intron1_65966
rs2715817	*MAPKK6*	T/C	Bin34	Intron1_71609
rs2715832	*MAPKK6*	T/C	Bin35	Intron10_4665
rs7761118	p38 MAP kinase	G/A	Bin1	Intron9_4460
rs2145362	p38 MAP kinase	C/G	Bin2	Intron3_2031
rs3752525	p38 MAP kinase	G/T	Bin3	Intron10_245
rs3730326	p38 MAP kinase	G/T	Bin4	Intron5_210
rs7770710	p38 MAP kinase	C/T	Bin5	Intron2_2152
rs16884694	p38 MAP kinase	G/A	Bin6	Intron8_18777
rs13196204	p38 MAP kinase	T/G	Bin7	Intron1_2726
rs3804453	p38 MAP kinase	A/G	Bin8	Exon12_542
rs3804454	p38 MAP kinase	T/G	Bin9	Intron1_10948
rs10807156	p38 MAP kinase	A/T	Bin10	Intron1_8809
rs4844550	*MAPKAPK2*	A/G	Bin1	5′flank_-882
rs10863784	*MAPKAPK2*	C/G	Bin2	Intron1_12931
rs12028997	*MAPKAPK2*	C/T	Bin3	Intron1_23505
rs4073250	*MAPKAPK2*	C/T	Bin4	Exon8_59
rs4072677	*MAPKAPK2*	T/G	Bin5	Intron1_20269
rs12060808	*MAPKAPK2*	C/T	Bin7	Intron1_18484
rs616589	*MAPKAPK3*	G/A	Bin1	Intron2_8414
rs3792323	*MAPKAPK3*	A/T	Bin2	Intron2_5116
rs3804628	*MAPKAPK3*	G/A	Bin3	Intron2_6866
rs2040397	*MAPKAPK3*	C/T	Bin4	Intron2_14863

Supplementary Table 2. Genotyping Results of 116 Tagging-SNPs

SNP	Gene	Alleles (1/2)	Group	All patients with HCV infection No. of genotypes (%) 1/1	1/2	2/2	Patients with HCV genotype 1b No. of genotypes (%) 1/1	1/2	2/2
rs2243594	*IFNAR1*	A/G	SR	210 (45.1)	213 (45.7)	43 (9.2)	94 (50.3)	93 (49.7)	20 (10.7)
			NR	263 (45.2)	245 (42.1)	74 (12.7)	198 (50.3)	176 (44.7)	55 (14)
rs2243600	*IFNAR1*	G/T	SR	128 (27.5)	223 (47.9)	115 (24.7)	62 (30)	101 (48.8)	44 (21.3)
			NR	163 (28)	300 (51.5)	120 (20.6)	119 (27.7)	217 (50.5)	94 (21.9)
rs2252930	*IFNAR1*	C/G	SR	298 (63.8)	152 (32.5)	17 (3.6)	125 (60.1)	75 (36.1)	8 (3.8)
			NR	362 (62.2)	191 (32.8)	29 (5)	274 (63.9)	134 (31.2)	21 (4.9)
rs2252650	*IFNAR2*	A/T	SR	145 (31)	227 (48.6)	95 (20.3)	63 (30.4)	101 (48.8)	43 (20.8)
			NR	168 (28.7)	293 (50)	125 (21.3)	119 (27.5)	219 (50.6)	95 (21.9)
rs6517154	*IFNAR2*	T/C	SR	413 (88.6)	50 (10.7)	3 (0.6)	181 (87.4)	24 (11.6)	2 (1)
			NR	509 (86.9)	76 (13)	1 (0.2)	378 (87.3)	54 (12.5)	1 (0.2)
rs2073362	*IFNAR2*	A/G	SR	338 (73)	116 (25.1)	9 (1.9)	149 (72.7)	52 (25.4)	4 (2)
			NR	452 (77.4)	121 (20.7)	11 (1.9)	341 (79.1)	84 (19.5)	6 (1.4)
rs2248202	*IFNAR2*	A/C	SR	183 (39.4)	210 (45.3)	71 (15.3)	80 (39)	96 (46.8)	29 (14.1)
			NR	218 (37.2)	274 (46.8)	94 (16)	155 (35.8)	205 (47.3)	73 (16.9)
rs10211925	*IFNAR2*	G/A	SR	436 (94.4)	26 (5.6)	0 (0)	189 (91.7)	17 (8.3)	0 (0)
			NR	553 (95.2)	27 (4.6)	1 (0.2)	412 (95.6)	18 (4.2)	1 (0.2)
rs2248412	*IFNAR2*	A/G	SR	269 (57.5)	166 (35.5)	33 (7.1)	114 (54.8)	81 (38.9)	13 (6.3)
			NR	313 (53.4)	232 (39.6)	41 (7)	228 (52.5)	177 (40.8)	29 (6.7)
rs310209	*JAK1*	C/A	SR	240 (51.6)	182 (39.1)	43 (9.2)	109 (52.7)	76 (36.7)	22 (10.6)
			NR	293 (49.9)	251 (42.8)	43 (7.3)	208 (47.9)	190 (43.8)	36 (8.3)
rs3790541	*JAK1*	C/T	SR	239 (51.2)	189 (40.5)	39 (8.4)	99 (47.6)	85 (40.9)	24 (11.5)
			NR	295 (50.5)	245 (42)	44 (7.5)	220 (50.8)	177 (40.9)	36 (8.3)
rs310247	*JAK1*	A/G	SR	147 (31.5)	233 (49.9)	87 (18.6)	72 (34.6)	105 (50.5)	31 (14.9)
			NR	180 (30.8)	295 (50.5)	109 (18.7)	140 (32.4)	220 (50.9)	72 (16.7)
rs3790532	*JAK1*	G/A	SR	252 (54.3)	175 (37.7)	37 (8)	114 (55.3)	74 (35.9)	18 (8.7)
			NR	317 (54)	232 (39.5)	38 (6.5)	224 (51.6)	176 (40.6)	34 (7.8)
rs2254002	*JAK1*	A/C	SR	158 (33.8)	230 (49.1)	80 (17.1)	74 (35.6)	106 (51)	28 (13.5)
			NR	186 (31.7)	304 (51.8)	97 (16.5)	145 (33.4)	225 (51.8)	64 (14.7)
rs3818753	*JAK1*	A/G	SR	405 (86.5)	59 (12.6)	4 (0.9)	173 (83.2)	31 (14.9)	4 (1.9)
			NR	532 (90.9)	53 (9.1)	0 (0)	389 (89.8)	44 (10.2)	0 (0)
rs17127024	*JAK1*	G/T	SR	310 (66.4)	134 (28.7)	23 (4.9)	141 (67.8)	56 (26.9)	11 (5.3)
			NR	369 (62.9)	194 (33)	24 (4.1)	276 (63.6)	142 (32.7)	16 (3.7)
rs2274948	*JAK1*	T/C	SR	358 (77)	98 (21.1)	9 (1.9)	154 (74.8)	48 (23.3)	4 (1.9)
			NR	424 (72.9)	153 (26.3)	5 (0.9)	312 (72.2)	115 (26.6)	5 (1.2)
rs280523	Tyrosine kinase2	G/A	SR	416 (89.3)	47 (10.1)	3 (0.6)	182 (87.9)	25 (12.1)	0 (0)
			NR	520 (88.6)	66 (11.2)	1 (0.2)	387 (89.2)	46 (10.6)	1 (0.2)
rs280519	Tyrosine kinase2	A/G	SR	134 (28.8)	241 (51.7)	91 (19.5)	58 (27.9)	113 (54.3)	37 (17.8)
			NR	166 (28.4)	293 (50.1)	126 (21.5)	130 (30)	208 (48)	95 (21.9)
rs280496	Tyrosine kinase2	C/G	SR	391 (83.5)	75 (16)	2 (0.4)	172 (82.7)	36 (17.3)	0 (0)
			NR	485 (82.6)	96 (16.4)	6 (1)	360 (82.9)	69 (15.9)	5 (1.2)
rs11885069	*STAT1*	C/T	SR	363 (78.1)	93 (20)	9 (1.9)	155 (75.2)	46 (22.3)	5 (2.4)
			NR	466 (79.5)	115 (19.6)	5 (0.9)	335 (77.4)	94 (21.7)	4 (0.9)
rs9789428	*STAT1*	C/A	SR	415 (88.7)	51 (10.9)	2 (0.4)	182 (87.5)	24 (11.5)	2 (1)
			NR	523 (89.4)	61 (10.4)	1 (0.2)	384 (88.9)	47 (10.9)	1 (0.2)
rs2280233	*STAT1*	T/C	SR	339 (72.6)	124 (26.6)	4 (0.9)	161 (77.8)	45 (21.7)	1 (0.5)
			NR	444 (75.8)	133 (22.7)	9 (1.5)	331 (76.4)	95 (21.9)	7 (1.6)
rs13395505	*STAT1*	A/G	SR	173 (37)	216 (46.3)	78 (16.7)	88 (42.5)	86 (41.5)	33 (15.9)
			NR	227 (38.7)	269 (45.8)	91 (15.5)	172 (39.6)	195 (44.9)	67 (15.4)
rs12693589	*STAT1*	C/T	SR	130 (27.8)	229 (48.9)	109 (23.3)	69 (33.2)	91 (43.8)	48 (23.1)
			NR	164 (27.9)	301 (51.3)	122 (20.8)	124 (28.6)	221 (50.9)	89 (20.5)
rs2066805	*STAT1*	T/C	SR	436 (93.2)	32 (6.8)	0 (0)	197 (94.7)	11 (5.3)	0 (0)
			NR	533 (91)	51 (8.7)	2 (0.3)	395 (91.2)	36 (8.3)	2 (0.5)
rs1400657	*STAT1*	T/G	SR	356 (76.1)	100 (21.4)	12 (2.6)	170 (81.7)	35 (16.8)	3 (1.4)
			NR	441 (75.3)	129 (22)	16 (2.7)	338 (78.1)	85 (19.6)	10 (2.3)
rs3771300	*STAT1*	T/G	SR	246 (52.6)	185 (39.5)	37 (7.9)	110 (52.9)	78 (37.5)	20 (9.6)
			NR	327 (56.2)	216 (37.1)	39 (6.7)	236 (54.9)	163 (37.9)	31 (7.2)
rs11677408	*STAT1*	C/T	SR	393 (84.2)	70 (15)	4 (0.9)	170 (82.1)	35 (16.9)	2 (1)
			NR	500 (85.3)	82 (14)	4 (0.7)	361 (83.4)	69 (15.9)	3 (0.7)
rs11887698	*STAT1*	A/G	SR	260 (55.6)	171 (36.5)	37 (7.9)	110 (52.9)	80 (38.5)	18 (8.7)
			NR	344 (58.6)	217 (37)	26 (4.4)	245 (56.5)	167 (38.5)	22 (5.1)

Supplementary Table 2. (Continued)

SNP	Gene	Alleles (1/2)	Group	All patients with HCV infection: No. of genotypes (%) 1/1	1/2	2/2	Patients with HCV genotype 1b: No. of genotypes (%) 1/1	1/2	2/2
rs2030171	*STAT1*	A/G	SR	214 (46.1)	202 (43.5)	48 (10.3)	105 (51)	80 (38.8)	21 (10.2)
			NR	268 (45.9)	252 (43.2)	64 (11)	203 (47.1)	181 (42)	47 (10.9)
rs1467199	*STAT1*	C/G	SR	119 (25.6)	236 (50.9)	109 (23.5)	44 (21.5)	101 (49.3)	60 (29.3)
			NR	162 (27.9)	286 (49.2)	133 (22.9)	115 (26.7)	215 (50)	100 (23.3)
rs10199181	*STAT1*	T/A	SR	231 (49.4)	189 (40.4)	48 (10.3)	115 (55.3)	75 (36.1)	18 (8.7)
			NR	286 (48.9)	245 (41.9)	54 (9.2)	222 (51.3)	174 (40.2)	37 (8.5)
rs2066802	*STAT1*	A/G	SR	288 (62.5)	149 (32.3)	24 (5.2)	128 (63.7)	64 (31.8)	9 (4.5)
			NR	373 (64)	179 (30.7)	31 (5.3)	271 (63)	136 (31.6)	23 (5.3)
rs16833155	*STAT1*	C/T	SR	436 (93.4)	31 (6.6)	0 (0)	196 (94.7)	11 (5.3)	0 (0)
			NR	531 (91.1)	50 (8.6)	2 (0.3)	394 (91.4)	35 (8.1)	2 (0.5)
rs2066799	*STAT1*	C/T	SR	391 (83.5)	70 (15)	7 (1.5)	169 (81.3)	35 (16.8)	4 (1.9)
			NR	496 (84.6)	86 (14.7)	4 (0.7)	358 (82.7)	72 (16.6)	3 (0.7)
rs11693463	*STAT1*	A/G	SR	338 (72.4)	118 (25.3)	11 (2.4)	148 (71.5)	53 (25.6)	6 (2.9)
			NR	419 (71.6)	153 (26.2)	13 (2.2)	303 (70)	119 (27.5)	11 (2.5)
rs10208033	*STAT1*	C/T	SR	208 (44.5)	212 (45.4)	47 (10.1)	95 (45.9)	92 (44.4)	20 (9.7)
			NR	276 (47.2)	254 (43.4)	55 (9.4)	201 (46.5)	191 (44.2)	40 (9.3)
rs3755312	*STAT1*	C/G	SR	336 (71.8)	118 (25.2)	14 (3)	142 (68.3)	57 (27.4)	9 (4.3)
			NR	447 (76.7)	127 (21.8)	9 (1.5)	317 (73.5)	107 (24.8)	7 (1.6)
rs2280232	*STAT1*	A/C	SR	337 (72.2)	119 (25.5)	11 (2.4)	157 (75.8)	46 (22.2)	4 (1.9)
			NR	397 (68)	171 (29.3)	16 (2.7)	295 (68.4)	125 (29)	11 (2.6)
rs13029532	*STAT1*	A/C	SR	354 (76.1)	102 (21.9)	9 (1.9)	165 (79.7)	38 (18.4)	4 (1.9)
			NR	426 (72.8)	145 (24.8)	14 (2.4)	322 (74.4)	99 (22.9)	12 (2.8)
rs7562024	*STAT1*	T/C	SR	370 (79.4)	94 (20.2)	2 (0.4)	174 (84.1)	32 (15.5)	1 (0.5)
			NR	459 (78.6)	116 (19.9)	9 (1.5)	349 (81)	76 (17.6)	6 (1.4)
rs1914408	*STAT1*	C/T	SR	218 (46.6)	195 (41.7)	55 (11.8)	86 (41.3)	92 (44.2)	30 (14.4)
			NR	249 (42.6)	264 (45.1)	72 (12.3)	189 (43.8)	191 (44.2)	52 (12)
rs2066807	*STAT2*	C/G	SR	424 (90.6)	43 (9.2)	1 (0.2)	189 (90.9)	18 (8.7)	1 (0.5)
			NR	523 (89.4)	60 (10.3)	2 (0.3)	392 (90.7)	40 (9.3)	0 (0)
rs12432194	IFN regulatory factor 9	C/T	SR	263 (56.4)	172 (36.9)	31 (6.7)	119 (57.5)	77 (37.2)	11 (5.3)
			NR	347 (59.1)	203 (34.6)	37 (6.3)	254 (58.5)	153 (35.3)	27 (6.2)
rs4981494	IFN regulatory factor 9	G/A	SR	202 (43.4)	211 (45.4)	52 (11.2)	95 (45.9)	91 (44)	21 (10.1)
			NR	272 (46.7)	250 (42.9)	61 (10.5)	197 (45.8)	187 (43.5)	46 (10.7)
rs12432304	IFN regulatory factor 9	C/T	SR	130 (27.9)	225 (48.3)	111 (23.8)	61 (29.5)	99 (47.8)	47 (22.7)
			NR	158 (27.2)	282 (48.6)	140 (24.1)	120 (28)	203 (47.4)	105 (24.5)
rs2277484	IFN regulatory factor 9	G/A	SR	337 (72.6)	110 (23.7)	17 (3.7)	154 (74.4)	45 (21.7)	8 (3.9)
			NR	401 (68.4)	170 (29)	15 (2.6)	295 (68)	127 (29.3)	12 (2.8)
rs2236350	IFN regulatory factor 9	C/A	SR	206 (44)	209 (44.7)	53 (11.3)	88 (42.3)	98 (47.1)	22 (10.6)
			NR	254 (43.6)	269 (46.1)	60 (10.3)	189 (43.8)	194 (44.9)	49 (11.3)
rs2303364	Ras-related C3 botulinum toxin substrate 1	C/T	SR	162 (34.8)	229 (49.2)	74 (15.9)	67 (32.5)	102 (49.5)	37 (18)
			NR	196 (33.7)	275 (47.3)	111 (19.1)	137 (31.9)	214 (49.8)	79 (18.4)
rs836483	Ras-related C3 botulinum toxin substrate 1	G/A	SR	384 (82.6)	76 (16.3)	5 (1.1)	171 (82.6)	35 (16.9)	1 (0.5)
			NR	472 (80.7)	110 (18.8)	3 (0.5)	346 (79.9)	84 (19.4)	3 (0.7)
rs6954996	Ras-related C3 botulinum toxin substrate 1	G/A	SR	412 (88.6)	51 (11)	2 (0.4)	182 (88.3)	23 (11.2)	1 (0.5)
			NR	513 (87.8)	68 (11.6)	3 (0.5)	377 (87.3)	52 (12)	3 (0.7)
rs7456834	Ras-related C3 botulinum toxin substrate 1	G/C	SR	307 (66)	144 (31)	14 (3)	133 (64.6)	62 (30.1)	11 (5.3)
			NR	370 (63.5)	197 (33.8)	16 (2.7)	270 (62.5)	151 (35)	11 (2.5)
rs702484	Ras-related C3 botulinum toxin substrate 1	G/C	SR	320 (68.5)	135 (28.9)	12 (2.6)	142 (68.3)	60 (28.8)	6 (2.9)
			NR	393 (67.2)	178 (30.4)	14 (2.4)	285 (66)	135 (31.3)	12 (2.8)
rs2347339	Ras-related C3 botulinum toxin substrate 1	C/G	SR	305 (65.3)	137 (29.3)	25 (5.4)	132 (63.8)	60 (29)	15 (7.2)
			NR	368 (63.1)	182 (31.2)	33 (5.7)	268 (62.2)	141 (32.7)	22 (5.1)
rs768409	Ras-related C3 botulinum toxin substrate 1	A/T	SR	456 (97.9)	10 (2.1)	0 (0)	202 (97.6)	5 (2.4)	0 (0)
			NR	579 (99.1)	5 (0.9)	0 (0)	428 (99.1)	4 (0.9)	0 (0)
rs2305871	*MAPKK3*	G/C	SR	241 (51.6)	202 (43.3)	24 (5.1)	104 (50.2)	89 (43)	14 (6.8)
			NR	317 (54.3)	223 (38.2)	44 (7.5)	233 (53.9)	164 (38)	35 (8.1)
rs9901404	*MAPKK3*	G/A	SR	207 (44.4)	212 (45.5)	47 (10.1)	97 (46.9)	93 (44.9)	17 (8.2)
			NR	232 (39.7)	271 (46.4)	81 (13.9)	180 (41.8)	193 (44.8)	58 (13.5)
rs12602109	*MAPKK3*	G/A	SR	167 (36)	224 (48.3)	73 (15.7)	76 (36.7)	94 (45.4)	37 (17.9)
			NR	238 (41.2)	265 (45.9)	74 (12.8)	174 (40.8)	193 (45.3)	59 (13.8)

Supplementary Table 2. (Continued)

SNP	Gene	Alleles (1/2)	Group	All patients with HCV infection No. of genotypes (%) 1/1	1/2	2/2	Patients with HCV genotype 1b No. of genotypes (%) 1/1	1/2	2/2
rs3760201	*MAPKK3*	A/G	SR	198 (42.6)	217 (46.7)	50 (10.8)	98 (47.3)	88 (42.5)	21 (10.1)
			NR	222 (38.5)	275 (47.7)	80 (13.9)	169 (39.4)	199 (46.4)	61 (14.2)
rs8074866	*MAPKK3*	C/T	SR	248 (53.2)	195 (41.8)	23 (4.9)	110 (53.1)	84 (40.6)	13 (6.3)
			NR	343 (58.9)	207 (35.6)	32 (5.5)	257 (59.6)	148 (34.3)	26 (6)
rs2074028	*MAPKK6*	T/C	SR	170 (36.5)	233 (50)	63 (13.5)	65 (31.3)	109 (52.4)	34 (16.3)
			NR	200 (34.2)	283 (48.4)	102 (17.4)	144 (33.3)	211 (48.8)	77 (17.8)
rs2034100	*MAPKK6*	G/A	SR	409 (87.6)	56 (12)	2 (0.4)	181 (87.4)	25 (12.1)	1 (0.5)
			NR	518 (88.7)	64 (11)	2 (0.3)	381 (88.2)	49 (11.3)	2 (0.5)
rs817565	*MAPKK6*	T/G	SR	125 (26.8)	214 (45.9)	127 (27.3)	66 (31.9)	87 (42)	54 (26.1)
			NR	159 (27.1)	284 (48.4)	144 (24.5)	115 (26.5)	216 (49.8)	103 (23.7)
rs2251862	*MAPKK6*	C/A	SR	231 (49.6)	193 (41.4)	42 (9)	88 (42.7)	95 (46.1)	23 (11.2)
			NR	263 (45)	259 (44.3)	62 (10.6)	186 (43)	198 (45.7)	49 (11.3)
rs2072073	*MAPKK6*	C/G	SR	239 (51.3)	183 (39.3)	44 (9.4)	112 (54.1)	76 (36.7)	19 (9.2)
			NR	272 (46.5)	264 (45.1)	49 (8.4)	204 (47.1)	196 (45.3)	33 (7.6)
rs2716213	*MAPKK6*	T/G	SR	159 (34)	222 (47.5)	86 (18.4)	58 (28)	103 (49.8)	46 (22.2)
			NR	201 (34.4)	274 (46.8)	110 (18.8)	140 (32.4)	202 (46.8)	90 (20.8)
rs12451722	*MAPKK6*	T/C	SR	304 (65.2)	145 (31.1)	17 (3.6)	141 (67.8)	56 (26.9)	11 (5.3)
			NR	382 (65.5)	177 (30.4)	24 (4.1)	283 (65.5)	129 (29.9)	20 (4.6)
rs6501326	*MAPKK6*	A/G	SR	187 (40.3)	216 (46.6)	61 (13.1)	76 (36.9)	96 (46.6)	34 (16.5)
			NR	231 (39.5)	268 (45.8)	86 (14.7)	167 (38.6)	204 (47.1)	62 (14.3)
rs2716225	*MAPKK6*	G/A	SR	345 (73.7)	108 (23.1)	15 (3.2)	152 (73.1)	46 (22.1)	10 (4.8)
			NR	437 (74.4)	141 (24)	9 (1.5)	336 (77.4)	93 (21.4)	5 (1.2)
rs8080760	*MAPKK6*	A/G	SR	143 (30.8)	233 (50.2)	88 (19)	62 (30.1)	105 (51)	39 (18.9)
			NR	177 (30.3)	294 (50.3)	114 (19.5)	131 (30.3)	213 (49.3)	88 (20.4)
rs12948059	*MAPKK6*	A/G	SR	341 (73.3)	112 (24.1)	12 (2.6)	160 (77.3)	43 (20.8)	4 (1.9)
			NR	418 (71.7)	153 (26.2)	12 (2.1)	323 (75.1)	100 (23.3)	7 (1.6)
rs2074027	*MAPKK6*	A/G	SR	156 (33.4)	223 (47.8)	88 (18.8)	79 (38)	92 (44.2)	37 (17.8)
			NR	206 (35.2)	264 (45.1)	115 (19.7)	156 (36)	188 (43.4)	89 (20.6)
rs2716222	*MAPKK6*	C/T	SR	186 (39.9)	217 (46.6)	63 (13.5)	86 (41.5)	93 (44.9)	28 (13.5)
			NR	260 (44.4)	244 (41.7)	81 (13.8)	194 (44.8)	180 (41.6)	59 (13.6)
rs4968857	*MAPKK6*	T/C	SR	144 (30.9)	232 (49.8)	90 (19.3)	77 (37.4)	88 (42.7)	41 (19.9)
			NR	192 (32.9)	275 (47.1)	117 (20)	143 (33.2)	205 (47.6)	83 (19.3)
rs756944	*MAPKK6*	T/C	SR	151 (32.5)	229 (49.2)	85 (18.3)	76 (37.1)	87 (42.4)	42 (20.5)
			NR	188 (32.2)	298 (51)	98 (16.8)	143 (33.2)	215 (49.9)	73 (16.9)
rs2715806	*MAPKK6*	G/A	SR	197 (42.5)	209 (45)	58 (12.5)	92 (44.4)	89 (43)	26 (12.6)
			NR	272 (46.5)	243 (41.5)	70 (12)	210 (48.6)	170 (39.4)	52 (12)
rs8078890	*MAPKK6*	A/C	SR	136 (29.2)	225 (48.3)	105 (22.5)	63 (30.4)	93 (44.9)	51 (24.6)
			NR	176 (30.1)	279 (47.8)	129 (22.1)	132 (30.6)	201 (46.6)	98 (22.7)
rs2716191	*MAPKK6*	C/T	SR	341 (73.3)	116 (24.9)	8 (1.7)	149 (72)	54 (26.1)	4 (1.9)
			NR	457 (78.3)	121 (20.7)	6 (1)	336 (77.8)	91 (21.1)	5 (1.2)
rs2715812	*MAPKK6*	C/T	SR	229 (49)	191 (40.9)	47 (10.1)	106 (51)	83 (39.9)	19 (9.1)
			NR	255 (43.6)	266 (45.5)	64 (10.9)	180 (41.7)	199 (46.1)	53 (12.3)
rs11869073	*MAPKK6*	A/C	SR	379 (81)	81 (17.3)	8 (1.7)	170 (81.7)	35 (16.8)	3 (1.4)
			NR	480 (81.8)	104 (17.7)	3 (0.5)	369 (85)	63 (14.5)	2 (0.5)
rs12945375	*MAPKK6*	A/G	SR	386 (82.7)	74 (15.8)	7 (1.5)	173 (83.6)	31 (15)	3 (1.4)
			NR	488 (83.1)	97 (16.5)	2 (0.3)	374 (86.2)	60 (13.8)	0 (0)
rs12939509	*MAPKK6*	A/G	SR	422 (90.2)	44 (9.4)	2 (0.4)	186 (89.4)	21 (10.1)	1 (0.5)
			NR	518 (88.2)	67 (11.4)	2 (0.3)	383 (88.2)	49 (11.3)	2 (0.5)
rs8082399	*MAPKK6*	G/A	SR	382 (81.8)	83 (17.8)	2 (0.4)	166 (79.8)	40 (19.2)	2 (1)
			NR	499 (85.4)	82 (14)	3 (0.5)	371 (86.1)	57 (13.2)	3 (0.7)
rs2716195	*MAPKK6*	G/A	SR	315 (67.7)	141 (30.3)	9 (1.9)	141 (68.4)	61 (29.6)	4 (1.9)
			NR	402 (68.7)	165 (28.2)	18 (3.1)	296 (68.5)	120 (27.8)	16 (3.7)
rs2716223	*MAPKK6*	G/A	SR	129 (27.7)	230 (49.4)	107 (23)	54 (26)	100 (48.1)	54 (26)
			NR	155 (26.5)	279 (47.7)	151 (25.8)	104 (24.1)	209 (48.4)	119 (27.5)
rs2715810	*MAPKK6*	G/A	SR	118 (25.3)	237 (50.7)	112 (24)	51 (24.6)	105 (50.7)	51 (24.6)
			NR	147 (25.1)	287 (49.1)	151 (25.8)	106 (24.5)	210 (48.6)	116 (26.9)
rs7213686	*MAPKK6*	T/C	SR	415 (88.9)	50 (10.7)	2 (0.4)	185 (89.4)	21 (10.1)	1 (0.5)
			NR	516 (87.9)	69 (11.8)	2 (0.3)	381 (87.8)	51 (11.8)	2 (0.5)

Supplementary Table 2. (Continued)

				All patients with HCV infection			Patients with HCV genotype 1b		
		Alleles		No. of genotypes (%)			No. of genotypes (%)		
SNP	Gene	(1/2)	Group	1/1	1/2	2/2	1/1	1/2	2/2
rs8067307	*MAPKK6*	C/A	SR	310 (66.4)	144 (30.8)	13 (2.8)	134 (64.7)	68 (32.9)	5 (2.4)
			NR	370 (63.1)	197 (33.6)	19 (3.2)	285 (65.7)	135 (31.1)	14 (3.2)
rs4968859	*MAPKK6*	A/C	SR	312 (67)	128 (27.5)	26 (5.6)	136 (65.4)	60 (28.8)	12 (5.8)
			NR	364 (62.2)	194 (33.2)	27 (4.6)	269 (62.3)	140 (32.4)	23 (5.3)
rs9893349	*MAPKK6*	G/A	SR	136 (29.3)	233 (50.2)	95 (20.5)	63 (30.6)	94 (45.6)	49 (23.8)
			NR	154 (26.3)	312 (53.2)	120 (20.5)	116 (26.8)	228 (52.7)	89 (20.6)
rs17690015	*MAPKK6*	G/A	SR	386 (82.7)	78 (16.7)	3 (0.6)	180 (87)	27 (13)	0 (0)
			NR	475 (81.2)	104 (17.8)	6 (1)	362 (83.8)	67 (15.5)	3 (0.7)
rs2715834	*MAPKK6*	G/C	SR	128 (27.4)	239 (51.2)	100 (21.4)	50 (24)	113 (54.3)	45 (21.6)
			NR	148 (25.3)	299 (51)	139 (23.7)	112 (25.9)	217 (50.1)	104 (24)
rs1548444	*MAPKK6*	T/G	SR	216 (46.6)	190 (40.9)	58 (12.5)	100 (48.8)	75 (36.6)	30 (14.6)
			NR	232 (39.8)	286 (49.1)	65 (11.1)	166 (38.6)	210 (48.8)	54 (12.6)
rs2715817	*MAPKK6*	T/C	SR	181 (38.7)	209 (44.7)	78 (16.7)	83 (39.9)	88 (42.3)	37 (17.8)
			NR	226 (38.6)	269 (45.9)	91 (15.5)	170 (39.3)	201 (46.4)	62 (14.3)
rs2715832	*MAPKK6*	T/C	SR	276 (59.2)	162 (34.8)	28 (6)	103 (49.8)	86 (41.5)	18 (8.7)
			NR	312 (53.4)	231 (39.6)	41 (7)	223 (51.7)	179 (41.5)	29 (6.7)
rs7761118	p38 MAP kinase	G/A	SR	398 (85.2)	67 (14.3)	2 (0.4)	175 (84.1)	32 (15.4)	1 (0.5)
			NR	494 (84.6)	86 (14.7)	4 (0.7)	366 (84.7)	64 (14.8)	2 (0.5)
rs2145362	p38 MAP kinase	C/G	SR	142 (30.5)	238 (51.2)	85 (18.3)	57 (27.5)	114 (55.1)	36 (17.4)
			NR	193 (32.9)	281 (48)	112 (19.1)	143 (33)	205 (47.3)	85 (19.6)
rs3752525	p38 MAP kinase	G/T	SR	254 (54.3)	192 (41)	22 (4.7)	107 (51.4)	89 (42.8)	12 (5.8)
			NR	319 (54.3)	226 (38.5)	42 (7.2)	233 (53.7)	169 (38.9)	32 (7.4)
rs3730326	p38 MAP kinase	G/T	SR	433 (92.5)	31 (6.6)	4 (0.9)	191 (91.8)	15 (7.2)	2 (1)
			NR	543 (92.7)	42 (7.2)	1 (0.2)	403 (93.1)	30 (6.9)	0 (0)
rs7770710	p38 MAP kinase	C/T	SR	418 (89.5)	49 (10.5)	0 (0)	190 (91.3)	18 (8.7)	0 (0)
			NR	544 (92.8)	40 (6.8)	2 (0.3)	398 (91.9)	35 (8.1)	0 (0)
rs16884694	p38 MAP kinase	G/A	SR	354 (76)	107 (23)	5 (1.1)	161 (77.4)	46 (22.1)	1 (0.5)
			NR	453 (77.8)	120 (20.6)	9 (1.5)	334 (77.7)	91 (21.2)	5 (1.2)
rs13196204	p38 MAP kinase	T/G	SR	293 (63)	164 (35.3)	8 (1.7)	122 (58.9)	81 (39.1)	4 (1.9)
			NR	387 (66.6)	170 (29.3)	24 (4.1)	282 (65.4)	132 (30.6)	17 (3.9)
rs3804453	p38 MAP kinase	A/G	SR	401 (85.9)	65 (13.9)	1 (0.2)	181 (87)	27 (13)	0 (0)
			NR	508 (86.8)	71 (12.1)	6 (1)	369 (85.4)	60 (13.9)	3 (0.7)
rs3804454	p38 MAP kinase	T/G	SR	364 (77.9)	93 (19.9)	10 (2.1)	162 (77.9)	39 (18.8)	7 (3.4)
			NR	451 (77.2)	124 (21.2)	9 (1.5)	338 (78.2)	89 (20.6)	5 (1.2)
rs10807156	p38 MAP kinase	A/T	SR	164 (35)	235 (50.2)	69 (14.7)	66 (31.7)	115 (55.3)	27 (13)
			NR	217 (37.3)	271 (46.6)	94 (16.2)	159 (36.7)	202 (46.7)	72 (16.6)
rs4844550	*MAPKAPK2*	A/G	SR	228 (49.1)	195 (42)	41 (8.8)	103 (49.5)	85 (40.9)	20 (9.6)
			NR	292 (50)	241 (41.3)	51 (8.7)	211 (49)	174 (40.4)	46 (10.7)
rs10863784	*MAPKAPK2*	C/G	SR	135 (29.2)	224 (48.4)	104 (22.5)	62 (30.4)	96 (47.1)	46 (22.5)
			NR	161 (27.4)	293 (49.9)	133 (22.7)	113 (26)	217 (50)	104 (24)
rs12028997	*MAPKAPK2*	C/T	SR	400 (85.5)	66 (14.1)	2 (0.4)	177 (85.1)	31 (14.9)	0 (0)
			NR	501 (85.5)	80 (13.7)	5 (0.9)	374 (86.4)	55 (12.7)	4 (0.9)
rs4073250	*MAPKAPK2*	C/T	SR	394 (84.9)	68 (14.7)	2 (0.4)	181 (87.9)	25 (12.1)	0 (0)
			NR	492 (84.4)	87 (14.9)	4 (0.7)	360 (83.7)	66 (15.3)	4 (0.9)
rs4072677	*MAPKAPK2*	T/G	SR	186 (39.9)	218 (46.8)	62 (13.3)	83 (40.1)	94 (45.4)	30 (14.5)
			NR	224 (38.2)	288 (49.1)	75 (12.8)	162 (37.3)	211 (48.6)	61 (14.1)
rs12060808	*MAPKAPK2*	C/T	SR	382 (81.8)	77 (16.5)	8 (1.7)	175 (84.5)	28 (13.5)	4 (1.9)
			NR	473 (81)	103 (17.6)	8 (1.4)	347 (80.5)	78 (18.1)	6 (1.4)
rs616589	*MAPKAPK3*	G/A	SR	215 (46)	205 (43.9)	47 (10.1)	111 (53.4)	84 (40.4)	13 (6.3)
			NR	235 (40.3)	271 (46.5)	77 (13.2)	164 (38)	209 (48.4)	59 (13.7)
rs3792323	*MAPKAPK3*	A/T	SR	242 (51.8)	187 (40)	38 (8.1)	124 (59.6)	75 (36.1)	9 (4.3)
			NR	273 (46.7)	253 (43.3)	58 (9.9)	189 (43.9)	196 (45.5)	46 (10.7)
rs3804628	*MAPKAPK3*	G/A	SR	416 (89.3)	48 (10.3)	2 (0.4)	184 (88.5)	22 (10.6)	2 (1)
			NR	519 (88.4)	66 (11.2)	2 (0.3)	389 (89.6)	43 (9.9)	2 (0.5)
rs2040397	*MAPKAPK3*	C/T	SR	288 (61.8)	155 (33.3)	23 (4.9)	124 (59.9)	74 (35.7)	9 (4.3)
			NR	393 (67)	170 (29)	24 (4.1)	282 (65)	132 (30.4)	20 (4.6)

NOTE. Genotype data are presented as the number of subjects with percentages in parentheses. Allele 1, major allele; Allele 2, minor allele.

Hepatology Research 2009; 39: 134–142 doi: 10.1111/j.1872-034X.2008.00416.x

Original Article

FDG positron emission tomography/computed tomography for the detection of extrahepatic metastases from hepatocellular carcinoma

Tomokazu Kawaoka,[1] Hiroshi Aikata,[1] Shintaro Takaki,[1] Kiminori Uka,[1] Takahiro Azakami,[1] Hiromi Saneto,[1] Soo Cheol Jeong,[1] Yoshiiku Kawakami,[1] Shoichi Takahashi,[1] Naoyuki Toyota,[2] Katsuhide Ito,[2] Yutaka Hirokawa[3] and Kazuaki Chayama[1]

[1]*Department of Medicine and Molecular Science, Division of Frontier Medical Science, Programs for Biomedical Research, Graduate School of Biomedical Sciences,* [2]*Department of Radiology, Hiroshima University and* [3]*Department of Radiology, Hiroshima Heiwa Clinic, Hiroshima, Japan*

Aims: To compare the efficacy of positron emission tomography (PET) computed tomography (CT), multi-detector helical computed tomography (MDCT) and bone scintigraphy for the detection of extrahepatic metastases in patients with hepatocellular carcinoma (HCC).

Methods: Thirty-four patients diagnosed with metastatic HCC were enrolled in this study. The lesions included lung ($n = 18$), bone ($n = 12$) and lymph node ($n = 16$) metastases. For receiver operating characteristic (ROC) analysis, lesions were diagnosed as metastatic HCC by two experienced abdominal radiologists. Another three physicians independently reviewed both positive and negative images. Each physician read three sets of images of MDCT, PET–CT and bone scintigraphy for bone metastasis.

Results: The mean sensitivity and specificity for diagnosis of lung metastasis were 85.2 and 88.9% for MDCT, and 59.2 and 92.6% for PET–CT, respectively. For lymph node metastasis, these values were 62.5 and 79.2% for MDCT, and 66.7 and 91.7% for PET–CT, respectively; and for bone metastasis 41.6 and 94.5% for MDCT, 83.3 and 86.1% for PET–CT, and 52.7 and 83.3% for bone scintigraphy, respectively. The mean Az values were 0.95 and 0.77 for MDCT and PET–CT in lung metastasis, respectively, 0.75 and 0.80 for MDCT and PET–CT for lymph node metastasis, respectively, and 0.59, 0.88 and 0.62 for MDCT, PET–CT and bone scintigraphy for bone metastasis, respectively.

Conclusion: PET–CT has high sensitivity and is more suitable for the detection of bone metastases from primary HCC, relative to MDCT and bone scintigraphy.

Key words: ^{18}F-FDG PET–CT, extrahepatic metastases from hepatocellular carcinoma, MDCT, ROC analysis, bone scintigraphy

INTRODUCTION

HEPATOCELLULAR CARCINOMA (HCC) is one of the most common cancers worldwide.[1] Since patients with HCC now live longer than before, thanks to improvements in diagnostic and therapeutic modalities, the number of patients with remote HCC metastases are increasing.[2] Various imaging techniques such as abdominal ultrasonography, multi-detector helical computed tomography (MDCT), computed tomography arterial portography (CTAP), CT during hepatic arteriography (CTHA) and magnetic resonance imaging (MRI) are useful tools for the detection and diagnosis of HCC.[3,4] MDCT, in contrast, is used as a tool for the detection of extrahepatic metastasis.[5] However, these imaging modalities fail to identify metastatic lesions in some patients.

^{18}F-fluoro-2-deoxy-D-glucose (^{18}F-FDG) positron emission tomography (PET) is a well-established, non-invasive diagnostic tool for the detection of a variety of malignant tumors such as neck, lung, pancreas and colon tumors.[6–8] However, ^{18}F-FDG PET is less suitable for the detection of primary HCC because of the variable ^{18}F-FDG uptake in HCC.[8] Nevertheless, a number of studies have used PET–CT for the detection of

Corresponding: Dr Hiroshi Aikata, Department of Medicine and Molecular Science, Division of Frontier Medical Science, Programs for Biomedical Research, Graduate School of Biomedical Sciences, Hiroshima University, 1-2-3 Kasumi, Minami-ku, Hiroshima 734-8551, Japan. Email: aikata@hiroshima-u.ac.jp
Received 14 May 2008; revision 8 July 2008; accepted 21 July 2008.

extrahepatic metastasis and reported its usefulness for this purpose.[9–11] To our knowledge, there are no studies that evaluated PET–CT for the diagnosis of extrahepatic metastases, especially using receiver operating characteristic (ROC) analysis. The multiple-reader ROC study design has become a frequently used tool in diagnostic radiology. With this tool, the investigator can characterize and compare the accuracy of diagnostic tests that rely on subjective interpretation.[12] The aims of the present study were to compare the efficacy of PET–CT as a tool for the detection of metastatic HCCs with MDCT by ROC analysis. For this purpose, we compared the Az value, sensitivity, specificity and positive predictive value of the MDCT and PET–CT for lung, lymph node and bone metastases originating from the liver.

METHODS

Patient population

^{18}F-FDG PET–CT AND MDCT were conducted in 34 consecutive patients diagnosed with extrahepatic metastases based on changes in size and changes in tumor marker between March 2005 and March 2007. In limited cases of bone metastases, bone scintigraphy was also conducted. These patients were enrolled as subjects of this study. Table 1 lists the patients' characteristics and location of extrahepatic metastases.

The primary tumor stage was evaluated according to the criteria of the Liver Cancer Study Group of Japan.[13] The sites of extrahepatic metastases were the lungs in 12 patients, lymph nodes in seven, bones in four, lungs and lymph nodes in three, lymph nodes and bones in five, lungs and bones in two and lungs, lymph nodes and bones in one patient. The total number of extrahepatic metastases was 18 in the lungs, 16 in lymph nodes and 12 in bones. Extrahepatic metastases were also detected in the adrenals in two patients, but these were not investigated due to the small number. There were no metastatic lesions in other organs.

Before performing PET–CT, the purpose of the diagnostic imaging was explained to each patient and written informed consent was obtained. The ethics committee did not require approval or informed consent for this retrospective study, which complied with the principles of the Helsinki Declaration.

Imaging methods

All examinations were performed within a 4-week interval.

Table 1 Characteristics of 34 patients with extrahepatic metastases

Age (years)*	59 (32–80)
Sex (male/female)	28/6
Etiology (HCV/HBV/HCV+HBV/others)	19/11/1/3
Intrahepatic tumor stage (T1/2/3/4)†	7/4/6/17
Child–Pugh score (A/B/C)	26/7/1
α-fetoprotein (ng/mL)*	904 (5–538 100)
Des-γ-carboxy prothrombin (mAU/mL)*	228 (12–645 250)
Site of extrahepatic metastases ($n = 34$)	
Lung/lymph/bone	12/7/4
Lung and lymph/lymph and bone/lung and bone	3/5/2
Lung and lymph and bone	1
Total number of extrahepatic metastases (lung/lymph/bone)	18/16/12
Size of extrahepatic metastases* (mm)	
Lung	9 (4–48)
Lymph	22 (12–87)
Bone	19 (5–120)

*Values are median (range).
†Based on the following three conditions (T factor): solitary, <2 cm in diameter, and no vessel invasion. T1 was defined as fulfilling the three conditions, T2 as fulfilling two of the three conditions, T3 as fulfilling one of the three conditions, T4 as fulfilling none of the three conditions.
HBV, hepatitis B virus; HCV, hepatitis C virus.

MDCT studies

MDCT involved scanning the patients from at least the base of the skull through to the pelvis. CT was first performed without a contrast medium to identify the liver. Using a DUAL SHOT power injector (Nemoto, Tokyo, Japan), 100 mL of iopamidol 300 (Iopamiron 300; Schering, Berlin, Germany) was injected at a rate of 3.5 mL/s through a 22-gauge catheter inserted into the antecubital vein. Four sets of images were acquired in a craniocaudal direction at 20, 40, 65 and 180 s after initiation of contrast medium injection. The first and second acquisitions were used for hepatic arterial phase images, the third acquisition for portal venous phase images, and the fourth acquisition for hepatic venous phase images. The third set of images was obtained during 20-s breath-holding, while those of the other acquisitions were achieved during 10-s breath-holding. All scans were performed on a LightSpeed Ultra 16 CT scanner (General Electric Medical Systems, Milwaukee, WI, USA) with scan parameters including 0.9-s gantry rotation speed, scan mode (20 mm Beam, Helical pitch 1.375), 1.25-mm slice thickness, 27.5 mm per rotation

table speed and reconstruction intervals of 0.625 mm for portal venous phase images.

^{18}F-FDG PET–CT studies

All PET scans were performed on a combined PET–CT system (Discovery ST; General Electric Medical Systems). The ^{18}F-fluoride was produced by an on-site cyclotron (HM12; Sumitomo Heavy Industry, Tokyo, Japan). ^{18}F-FDG was synthesized by the automated Hamacher method and tested for sterility, pyrogenicity and radiochemical purity on each production run. All patients were fasted for at least 5 h before injection of 300–400MBq ^{18}F-FDG. Imaging commenced 1 h after injection. Scanning included the area from at least the base of the skull through to the femoral region, applying a three-dimensional mode with a 1.5 min acquisition per bed position. All studies were reconstructed using default vender-implemented iterative reconstruction algorithm.

Bone scintigraphy studies

For bone scintigraphy, technetium-99m methylene diphosphonate was injected at a dose of 555 MBq (^{15m}Ci)-740 MBq (^{20m}Ci), and imaging begun 2 h after injection. Examinations were performed with a large-field-of-view gamma camera, with a high-resolution collimator. Multiple overlapping spot images were obtained of the entire body.

Image analysis

The obtained images were analyzed before the pathologic results became known, and were presented in a random order. Before performing ROC analysis, two experienced radiologists (Y. H., K. I.), who served as the study coordinators in the ROC analysis, defined the gold standard. They were given the images obtained from the above imaging modalities, including MDCT, ^{18}F-FDG PET–CT and bone scintigraphy, as well as the operative, laboratory and histological findings. They defined the gold standard by the appearance of mass lesion from those not detected previously, worsening of HCC, increase in tumor size, increase in tumor marker and histological finding.

Ten patients later underwent autopsy and two patients underwent surgery for lung tumor. Another group of three gastroenterologists (H. A., K. U., S. T) with a specialty in imaging diagnosis who had at least 10 years' experience in interpreting MDCT and bone scintigraphy and 3 years' experience in interpreting ^{18}F-FDG PET–CT images in their practices, independently reviewed the three sets of images (MDCT, fusion images of ^{18}F-FDG PET–CT and bone scintigraphy). The databases of all images were also used as the reference libraries (online atlases) for our intelligent workstation.

These gastroenterologists were informed that the patients had HCCs and had been referred for pretherapeutic assessment of suspected metastasis, but knew nothing else about the patients. To minimize learning bias, the reviewing order was randomized and the reviewing procedure was conducted in four sessions at 2-week intervals. Three gastroenterologists, one for each modality, read the MDCT, fusion images of ^{18}F-FDG PET–CT and bone scintigraphy separately and prospectively at each participating site. In the above analyses, the same numbers of patients that did not have HCC metastasis were included as negative images (lung/lymph/bone = 18/16/12).

On PET–CT images, a region of interest (ROI) was drawn over the areas of maximum intensity in each lesion for semi-quantitative analysis. The ROI data were processed as a standardized uptake value (SUV). Lesions were identified as positive if the accumulation of ^{18}F-FDG was higher than a normal contralateral structure or surrounding tissues. A lack of increased activity was considered a normal finding.

Each reader scored each image for the presence of metastatic HCC lesions and assigned confidence levels to his observation (1 = definitely negative, 2 = probably negative, 3 = possibly positive, 4 = probably positive, 5 = definitely positive).

Statistical analysis

For each imaging technique, a binomial ROC curve was fitted to each observer's confidence rating data by maximum likelihood estimation with a ROC analysis program (ROCKIT 0.9.1B; Metz CE, Chicago, IL, USA).[14] The diagnostic accuracy of each imaging technique was determined by calculating the area (Az) under each observer-specific binomial ROC curve when it was plotted in the designated square. Composite ROC curves representing the performance of all physicians as a single observer were obtained for each pair of imaging sequences using the maximum likelihood curve-fitting algorithm to rate the pooled data of the three independent physicians. A P value less than 0.05 was considered to represent statistically significant difference. The relative sensitivities of each imaging modality for detection by three individual observers and extrahepatic metastases composite data were determined using the number of assigned score of 4 or more for extrahepatic metastases.

Table 2 Az value, sensitivity, specificity and positive predictive value in detection of lung metastasis

Observer	Az value		Sensitivity (%)		Specificity (%)		Positive predictive value (%)	
	MDCT	PET–CT	MDCT	PET–CT	MDCT	PET–CT	MDCT	PET–CT
1	0.956	0.691	88.9	55.6	94.4	94.4	94.1	100.0
2	0.957	0.807	77.8	72.2	94.4	88.9	93.3	100.0
3	0.938	0.814	88.9	50.0	88.9	94.4	88.9	100.0
Mean	0.950	0.771	85.2	59.2	88.9	92.6	92.1	100.0
P value*		0.054		0.128		1.0		0.039

*Compared with the value for MDCT.
MDCT, multi-detector helical computed tomography; PET–CT, positron emission tomography – computed tomography.

The specificity of each imaging modality was determined by the number of assigned score of 3 or less without extrahepatic metastases. The relative sensitivities and specificities of each imaging modality were compared using the McNemar test. To assess inter-observer variability in interpreting images, kappa statistics were used to measure the degree of agreement between observers.[15] A kappa value greater than 0 was considered to indicate a positive correlation. Values up to 0.4 were considered to indicate positive but poor correlation; values of 0.41–0.75, good correlation; and values greater than 0.75, excellent correlation.

RESULTS

Lung metastasis

THREE OBSERVERS ACHIEVED a slightly lower diagnostic performance on PET–CT images than MDCT, but the difference in the mean Az values of both image sets was not significant. The positive predictive value for analysis of MDCT was significantly lower than that of PET–CT for all observers (Table 2, Fig. 1a). False negative lesions in PET–CT were 16.7% (3/18). The PET–CT showed no accumulation of ^{18}F-FDG in both metastatic lesions and in primary lesions of HCC in three cases. The tumor size of these three cases was 3, 5 and 8 mm, respectively. The images of one of these patients are shown in Figure 2.

Lymph node metastasis

There were no significant differences between analyses of MDCT and PET–CT images for all observers in the Az value, sensitivity, specificity and positive predictive values (Table 3, Fig. 1b). False negative lesions in PET–CT were 6.3% (1/16). The PET–CT showed no accumulation of ^{18}F-FDG in both the metastatic lesions and primary lesions of HCC in one case. Figure 3 shows that the lymphadenopathy detected by MDCT was considered to be benign lesion due to no accumulation of ^{18}F-FDG.

Bone metastasis

The Az value and sensitivity were higher on PET–CT images than MDCT (mean Az, 0.883 and 0.594, respectively; $P = 0.027$, mean sensitivity, 83.3 and 41.6%,

Table 3 Az value, sensitivity, specificity and positive predictive value in detection of lymph node metastasis

Observer	Az value		Sensitivity (%)		Specificity (%)		Positive predictive value (%)	
	MDCT	PET–CT	MDCT	PET–CT	MDCT	PET–CT	MDCT	PET–CT
1	0.794	0.824	50.0	62.5	87.5	87.5	80.0	83.3
2	0.683	0.842	50.0	68.8	87.5	93.8	80.0	91.7
3	0.787	0.761	87.5	68.8	62.5	93.8	70.0	100.0
Mean	0.755	0.809	62.5	66.7	79.2	91.7	76.7	91.7
P value*		0.425		0.752		0.335		0.197

*Compared with the value for MDCT.
MDCT, multi-detector helical computed tomography; PET–CT, positron emission tomography – computed tomography.

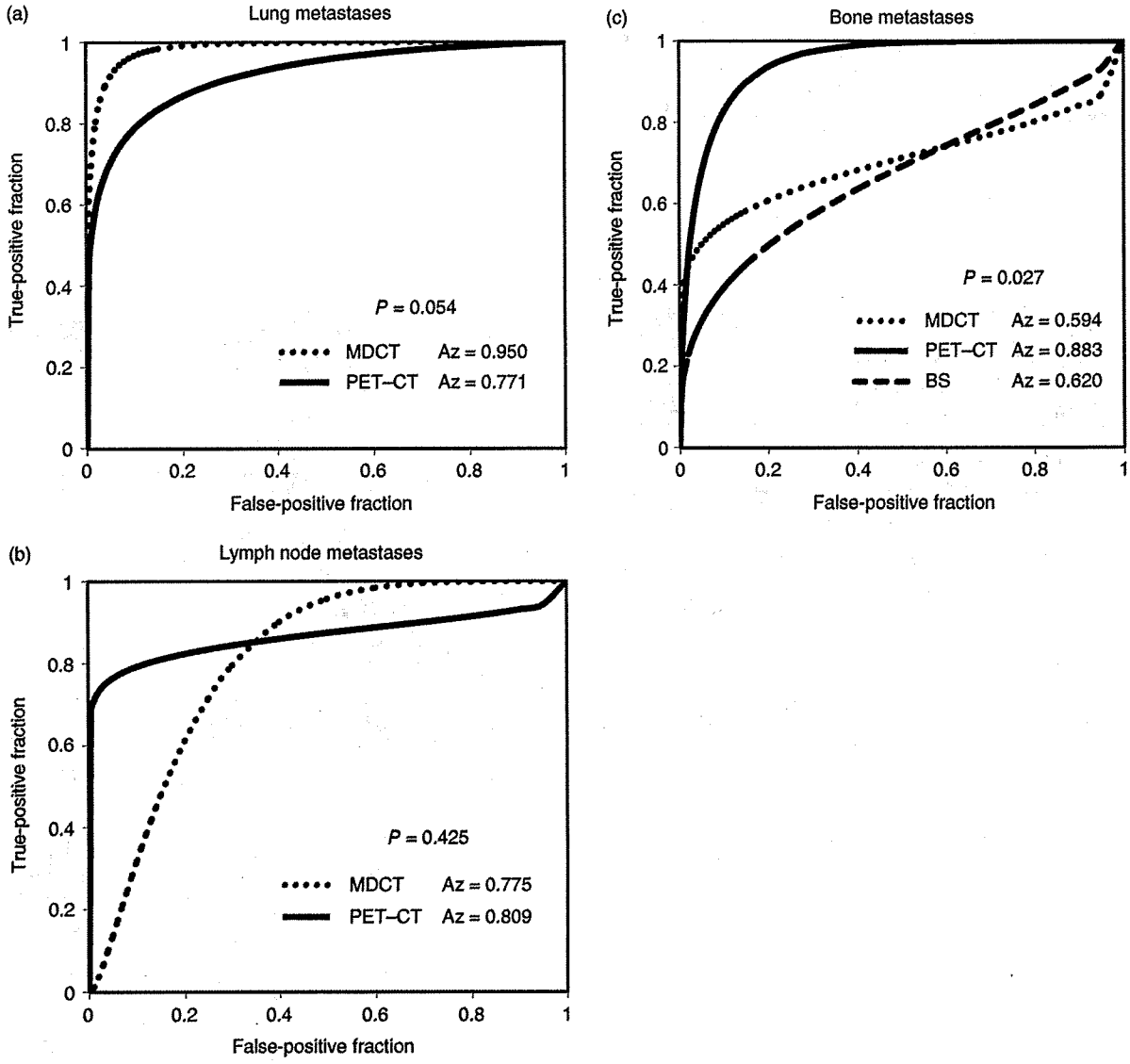

Figure 1 Receiver operating characteristic (ROC) curves for (a) lung metastases, (b) lymph node metastases and (c) bone metastases using data of all observers.

respectively; $P = 0.002$). However, there were no significant differences in specificity and positive predictive value between analysis of MDCT and PET–CT images for all observers. The sensitivity of PET–CT in detecting bone metastases from primary HCC tended to be higher than bone scintigraphy (83.3 and 52.7%, respectively; $P = 0.053$). Furthermore, the Az value of PET–CT was higher than bone scintigraphy (0.883 and 0.620, respectively; $P = 0.027$, Table 4, Fig. 1c).

False negative lesions were 16.7% (2/12) in MDCT and 0% in PET–CT (Fig. 4a,b). These two lesions which could not be detected by MDCT were clearly detected by PET-CT, showed the accumulation of ^{18}F-FDG and were not detected by bone scintigraphy (Fig. 4c).

The mean kappa values were 0.42, 0.45 and 0.52 for lung metastases, lymph node metastases and bone metastasis, respectively. All kappa values were considered to represent good correction.